AD-A032 318 SAINT LOUIS UNIV MO DEPT OF EARTH AND ATMOSPHERIC S--ETC F/G 4/2
RESEARCH TO DEVELOP IMPROVED MODELS OF CLIMATOLOGY THAT WILL AS--ETC(U)
AUG 76 D E MARTIN F19628-74-C-0004

UNCLASSIFIED AFGL-TR-76-0249 NL

| OF |
AD
A032 318

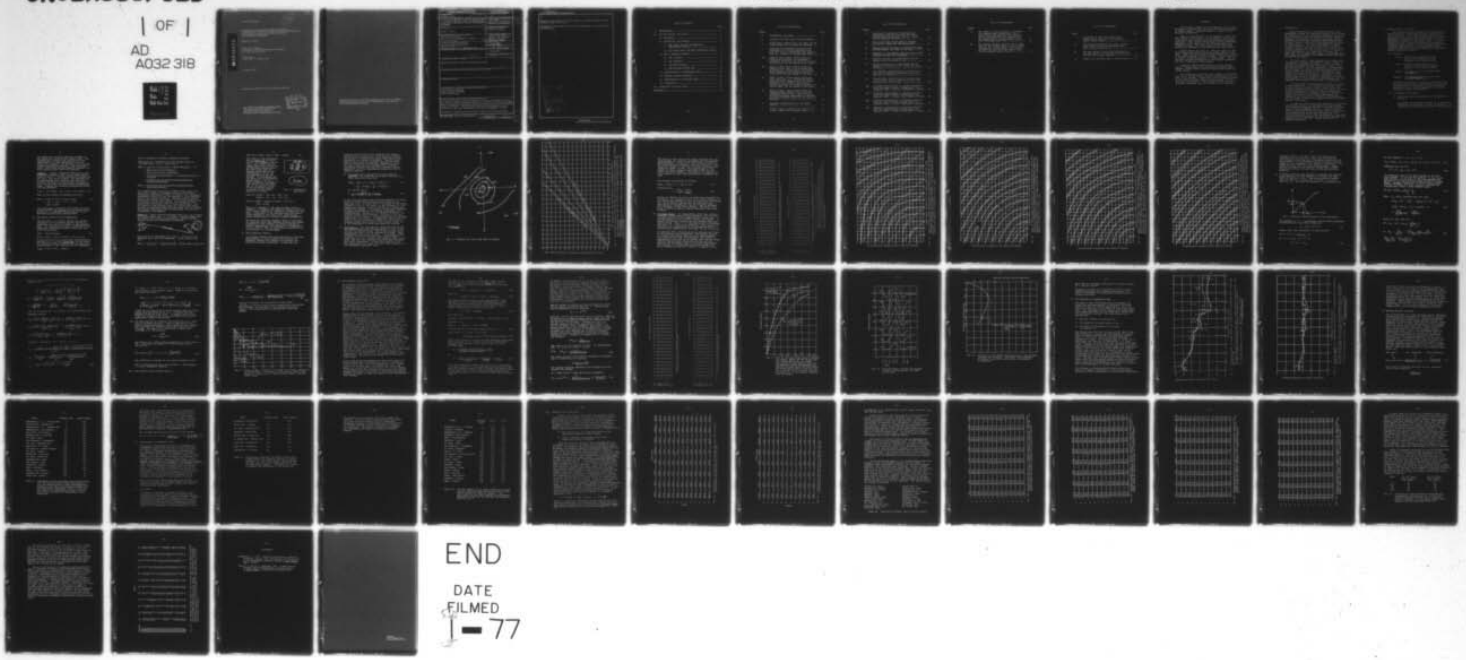

END

DATE
FILMED
1-77

AFGL-TR-76-0249

(12)

FC

RESEARCH TO DEVELOP IMPROVED MODELS OF CLIMATOLOGY THAT WILL ASSIST THE METEOROLOGIST IN THE TIMELY OPERATION OF THE AIR FORCE WEATHER DETACHMENTS

AD A032318

Donald E. Martin

Saint Louis University
Department of Earth and Atmospheric Sciences
St. Louis, Missouri 63103

Final Report
1 July 1975 - 31 August 1976

31 August 1976

Approved for public release; distribution unlimited

DDC
RECEIVED
NOV 23 1976
B

AIR FORCE GEOPHYSICS LABORATORY
AIR FORCE SYSTEMS COMMAND
UNITED STATES AIR FORCE
HANSCOM AFB, MASSACHUSETTS 01731

Qualified requestors may obtain additional copies from the Defense Documentation Center. All others should apply to the National Technical Information Service.

UNCLASSIFIED
SECURITY CLASSIFICATION OF THIS PAGE (When Data Entered)

REPORT DOCUMENTATION PAGE

READ INSTRUCTIONS BEFORE COMPLETING FORM

1. REPORT NUMBER: AFGL-TR-76-0249	2. GOVT ACCESSION NO.
3. RECIPIENT'S CATALOG NUMBER	
4. TITLE (and Subtitle): RESEARCH TO DEVELOP IMPROVED MODELS OF CLIMATOLOGY THAT WILL ASSIST THE METEOROLOGIST IN THE TIMELY OPERATION OF THE AIR FORCE WEATHER DETACHMENTS.	5. TYPE OF REPORT & PERIOD COVERED: Final Report. 1 Jul 75 - 31 Aug 76. Covers life of contract.
	6. PERFORMING ORG. REPORT NUMBER
7. AUTHOR(s): Donald E. Martin	8. CONTRACT OR GRANT NUMBER(s): F19628-74-C-0004
9. PERFORMING ORGANIZATION NAME AND ADDRESS: Saint Louis University, Dept. of Earth and Atmospheric Sciences, St. Louis, MO 63103	10. PROGRAM ELEMENT, PROJECT, TASK AREA & WORK UNIT NUMBERS: Project, Task, Work Unit 86240201, DOD 62101F Sub Element 688624
11. CONTROLLING OFFICE NAME AND ADDRESS: Air Force Geophysics Laboratory, Hanscom AFB, MA. 01731, Contract Monitor: I. I. Gringorten, LYK	12. REPORT DATE: 31 Aug 1976
	13. NUMBER OF PAGES: 55 (56 pp.)
14. MONITORING AGENCY NAME & ADDRESS (if different from Controlling Office)	15. SECURITY CLASS. (of this report): Unclassified
	15a. DECLASSIFICATION/DOWNGRADING SCHEDULE

16. DISTRIBUTION STATEMENT (of this Report)

Approved for public release; distribution unlimited.

17. DISTRIBUTION STATEMENT (of the abstract entered in Block 20, if different from Report)

18. SUPPLEMENTARY NOTES

19. KEY WORDS (Continue on reverse side if necessary and identify by block number)

Unconditional Climatology
Mission Success Indicators
Joint Probabilities

20. ABSTRACT (Continue on reverse side if necessary and identify by block number)

This research provides a means of modelling the joint relationships of ceiling and visibility probabilities among stations as a function of distance and season. Analytic formulations are presented which show definite skill over the assumption of data independency. These functions carry the added advantage of being applicable for any route irrespective of direction, topography or location.

A preliminary attempt has also been made to compact the unconditional prob- → next page

DD FORM 1 JAN 73 1473 EDITION OF 1 NOV 65 IS OBSOLETE

UNCLASSIFIED
SECURITY CLASSIFICATION OF THIS PAGE (When Data Entered)

405 292

20.

abilities at any station for limited elements into forms amenable for rapid computer storage and retrieval.

Discussions of the results, verifications and approaches to the above topics are presented.

TABLE OF CONTENTS

		Page
I.	INTRODUCTION	1
II.	MISSION SUCCESS INDICATORS	2
	1) NOTATIONS	2
	2) DEFINITIONS AND EXAMPLES	2
	a) CMSI BASED UPON THE ASSUMPTION OF INDEPENDENCY ($CMSI_i$)	2
	b) CMSI WHICH ALLOW FOR DATA DEPENDENCIES $CMSI_t$	3
	3) CMSI MODELLING EFFORTS	5
	a) THE K-FACTOR	6
	b) THE M-FACTOR	6
	c) THE ALPHA FACTOR	9
	d) THE BILLIKEN FACTOR (BF)	20
	4) VERIFICATIONS ON INDEPENDENT DATA	27
	5) REVISED ANALYTIC FUNCTIONS	30
	6) VERIFICATIONS ON DEPENDENT DATA	32
	7) CONCLUSION	32
III.	MODELLING THE RUSSWO DATA	36
REFERENCES		47

List of Illustrations

Figure		Page
1	Intersection and union.....	5
2	K-factors for 0000 Local Time in January....	7
3	Relationship between $CMSI_t$ and $CMSI_i$ for the winter season as a function of distance	8
4	M-factors for expressing meteorological homogeneity for ceiling conditions less than 200' and/or visibilities less than 1/2 mile as a function of distance and month.....	10
5a	Graph of $CMSI_t$ (heavy curved lines) for Lakenheath-Mildenhall and Mildenhall-Lakenheath comprising the distance interval of 0-50 miles for all months of the year....	11
5b	Graph of $CMSI_t$ (heavy curved lines) for Ramstein-Rhein Main, Rhein Main-Ramstein Dover-McGuire, McGuire-Dover and Andrews-Dover comprising the distance interval of 50-100 miles for all months of the year.....	12
5c	Graph of $CMSI_t$ (heavy curved lines) for Pope-Charleston, S.C., Charleston-Robins, Robins-Dobbins, Benning-Robin, Ft. Hood-Bergstrom, Altus-Tinker, and Dobbins-Robins comprising the distance interval of 100-200 miles for all months of the year...	13
5d	Graph of $CMSI_t$ (heavy curved lines) for Travis-Alameda, Hill-Mt. Home, Eielson-Elmendorf, Rota-Torrejon, Moron-Torrejon and Torrejon-Moron comprising the distance interval of 200-300 miles for all months of the year.....	14
6	Schematic representation of the Alpha-factor.....	15
7	Values of α as a function of distance for winter, summer and the annual mean.....	19

List of Illustrations

Figure		Page
8	B-Factors for expressing meteorological homogeneity ceilings less than 200' and/or visibilities less than 1/2 mile as a function of distance and month.....	23
9	Plot of Billiken factor against distance for winter, summer and the annual mean.....	24
10	Billiken-factor isolines for constant mileages plotted against the month of the year.....	25
11	Variation of the maximum amplitude term of the Billiken function with distances.....	26
12	Relative accuracy of the α-method and BF-method during the month of Jan.	28
13	Relative accuracy of the α-method and BF-method for estimating CMSI during the month of April.....	29
14	Unconditional probabilities of ceilings less than 1000 ft and/or visibilities less than one mile at Otis AFB.....	37
15	Unconditional probabilities of ceilings less than 500 feet and/or visibilities less than one-half mile at Otis AFB.	38
16a	Estimated probabilities of ceiling/visibility 200/½ for upper Heyford, England using the equation $P200/\frac{1}{2} = P500/\frac{1}{2} + B_1(P1000/1 - P500/\frac{1}{2})$.	40
16b	Estimated probabilities of ceiling/visibility 200/¼ for upper Heyford, England using the equation $P200/\frac{1}{4} = P500/\frac{1}{2} + B_2 (P1000/1 - P500/\frac{1}{2})$.	41
16c	Estimated probabilities of ceiling/visibility 800½ for upper Heyford, England using the equation $P800/\frac{1}{2} = P500/\frac{1}{2} + B_3(P1000/1 - P500/\frac{1}{2})$.	42
16d	Estimated probabilities of ceiling/visibility 800¼ for upper Heyford, England using the equation $P800/\frac{1}{4} = P500/\frac{1}{2} + B_4(P1000/1 - P500/\frac{1}{2})$.	43

List of Illustrations

Figure		Page
17	The number of types required to reproduce the unconditional probabilities for a given RUSSWO ceiling/visibility category for an unlimited number of stations for all months within a given maximum allowable percentage error (PC).....	44
18	The numbers indicate which of the 31 types best fit the diurnal profile of the listed stations for a given month. The criteria are ceilings less than 500' and/or visibilities greater than 1/2 mile.....	46

List of Illustrations

Table		Page
I	Percentage of times when $CMSI_i$ gave larger errors than the Billiken-factor method during winter.....	31
II	Verification statistics for select routes which helped provide the original data used to devise equation 31.	33
III	The mean errors (in per cent) between the revised analytic Billiken-factor method and the true CMSI during January.....	35
IV	Twenty five stations used in initial study.....	39

PERSONNEL

The following members of the Department of Earth and Atmospheric Sciences were engaged in the research program at various stages. Professor Donald E. Martin was the Principal Investigator.

James P. Long did much of the pioneering work on the CMSI portion of the report. He was aided by John Riess, Terry Phelps and William Talman in devising the analytic functions. James Wilson and Lorraine Stickel contributed materially to all aspects of this research during its formative stages. The verification of the CMSI formulations was performed by Dale Johnson and George Jacroux.

Robert Bishop and James St. John were active in the RUSSWO modelling efforts during the early stages of that work. Frank Holt and Richard Picanso advanced this effort to the point reported in this document. Eloise Myers and Al Kreiner conducted research in various areas. The regression equation formulations of this report represents but one of their many contributions.

Numerous students participated on a less extended basis. Primary among these were Ron Przbylinski, Gene Arbogast, Robert Thiele, Harvey Ferdman, Alan Kikawa and Gordon Neithe.

Mr. Gringorten of AFGL was very helpful in reviewing this report and providing valuable contributions with regard to its content. Albert Boehm of AWS provided guidance to the project through frequent consultations with the Principal Investigator. Mrs. Frances Brummell served as secretary throughout the entire course of the research.

I. INTRODUCTION

Recent innovations in Air Weather Services have emphasized the need for modelling climatic data in order to transfer much of the information presently stored in book or page form into the computer for rapid retrieval purposes. This presents a host of challenges to the statistically-oriented, meteorologically-knowledgeable scientist since he has very little precedence to follow in these efforts. Since this combination of talents is rather unique to any given individual, a team of students working under the guidance of Professor Martin has been assembled to attack the problem. In addition, a CMSI coordinating team comprised of experts from AFGL, AWS and SLU meets twice yearly to guide the overall effort and supplement the talents of the Saint Louis University contingent.

The first goal of this research was to model joint ceiling and visibility relationships among stations as a function of distance and season. We have systematically progressed through four phases, each of which has definite merit over the assumption of independency. The end result is a simple modelling method which presents a ready estimation of joint probabilities as a function of season and distance. The analytic formulations which we have devised are applicable for any route irrespective of direction, topography or location. Verification of these methods on both dependent and independent data attest to their merit and simplicity.

A second phase of the research involved the problem of data compaction. The unconditional probabilities, in particular, represent a massive array which would quickly saturate the largest of computer storage systems. By taking advantage of inherent joint relationships among the statistics of adjacent points in the RUSSWO, diurnal and annual imposed trends, and through the application of analysis compartmentization techniques, we have found it possible to compact the data by several orders of magnitude.

To date our efforts have been confined to categories which carry combined ceiling/visibility restrictions. The procedures developed pertain to separate considerations of these parameters as well. Thus, we plan to process the ceiling/visibility data (either separately or in combinations as the need requires) for some 360 stations where RUSSWO data are available. This will offer an on-line capability for retrieving unconditional probability data for "any" desired point over the Northern Hemisphere.

II. MISSION SUCCESS INDICATORS

The mission success indicator (MSI) specifies the probability that a particular mission can be successfully completed. Since many factors in addition to weather often enter into its calculations, our research represents a restricted version of the MSI. It will henceforth be denoted by the symbol, CMSI. It is the probability that a specific mission will experience favorable weather conditions based entirely upon climatological considerations. Such information offers valuable inputs into both the planning and operational phases of military missions.

1) Notations

$P(Au)$ = Unconditional probability that point A is up (above specified minimums) at the desired time.

$P(Bd)$ = Unconditional probability that point B is down (below specified minimums) at the desired time.

$PAdUBd$ = The union of the two unconditional probabilities.

$P(Au \wedge Bu)$ = The intersection of the two unconditional probabilities.

By definition, $P(Au) = 1 - P(Ad)$. Thus whether the available unconditional probabilities for a station are presented as being above or below minimums is immaterial since a simple conversion can be made from one statistic to the other.

2) Definitions and Examples

a) CMSI Based Upon the Assumption of Independency ($CMSI_i$)

One method for producing the CMSI is to assume independency and multiply together the respective unconditional probabilities that each station used in

the flight will be above specified minimums at the appropriate take-off and landing times. The unconditional probabilities required for such computations have been tabulated by hour (or other time increment) for virtually all air bases, airports and weather stations. They have been widely distributed and are commonly available for most locations where CMSI's are desired.

Example 1. Assume a departure from point A, with stopovers at points B and C, and a final destination at point D. Ceiling/visibility minimums are 500 ft/1.0 mile at all points. The stopovers are of sufficiently short duration that the unconditional probability of being above minimums at B and C are the same for both arrival and departure times. Suppose the following unconditional probabilities pertained:

$$P(Au) = .85 \quad P(Bu) = .80 \quad P(Cu) = .67 \quad P(Du) = .72$$

Then, by this method of computing the $CMSI_i$,

$$CMSI_i = P(Au) \times P(Bu) \times P(Cu) \times P(Du) \qquad (1)$$
$$= .85 \times .80 \times .67 \times .72$$
$$= .328 = 32.8\%$$

This represents a perfectly valid method of calculating the CMSI IF, AND ONLY IF the unconditional probability at each point is independent of all the other unconditional probabilities.

b) CMSI which Allow for Data Dependencies

The true CMSI, i.e., $CMSI_t$, denotes the climatic probability of a successful mission whereby no assumptions are made with regard to data dependencies. Its calculation requires a knowledge of the respective unconditional probabilities and their joint relationships.

$$CMSI_t = P(Au_\wedge Bu_\wedge Cu_\wedge Du). \qquad (2)$$

$$CMSI_t = CMSI_i = P(Au) \times P(Bu) \times P(Cu) \times P(Du)$$

if, and only if, the unconditional probabilities of stations A, B, C, D are independent of each other. The following formula pertains when the respective unconditionals of two stations are not independent

$$P(X_\wedge Y) = P(X) + P(Y) - P(XUY). \qquad (3)$$

This is extended to several stations as follows:

(Here A,B,C,D = probability of that station being up at right time, i.e. A = P(Au), etc.)

$$CMSI_t = A \wedge B \wedge C \wedge D = [(A \wedge B) \wedge C] \wedge D = [(A+B-AUB) \wedge C] \wedge D \quad (4)$$

$$= [(A+B-AUB)+C-(A+B-AUB)UC] \wedge D$$

$$= [(A+B-AUB+C-AUC-BUC-AUBUC)] \wedge D$$

$$= (A+B-AUB+C-AUC-BUC+AUBUC) + D -(A+B-AUB+C-BUC-AUC+ AUBUC)UD$$

$$= A+B-AUB+C-AUC-BUC+AUBUC+D-AUD-BUD+AUBUD-CUD +AUCUD+BUCUD-AUBUCUD.$$

$$CMSI_t = A+B+C+D-AUB-AUC-BUC-AUD-BUD-CUD+AUBUC+AUBUD+ AUCUD+BUCUD-AUBUCUD .$$

It is readily seen that the true CMSI becomes quite complex when a number of dependent stations is involved. Statistical evaluation of $CMSI_t$ by "brute force" sequential processing of data for just two stations is time consuming even on the fastest computers. Processing multi-station routes with variable lag times on a real time request basis is virtually out of the question. The effects of data dependencies essentially work to make $CMSI_t \geq CMSI_i$. The net result is most apparent when the unconditional probabilities of restricted conditions are large and the stations are located relatively close to each other. This will be illustrated by an example.

Example 2. Assume that the distance from A to B is 50 miles, B to C 400 miles, and C to D 25 miles. Further assume (for the moment) that stations separated by distances greater than 200 miles have independent climatology.

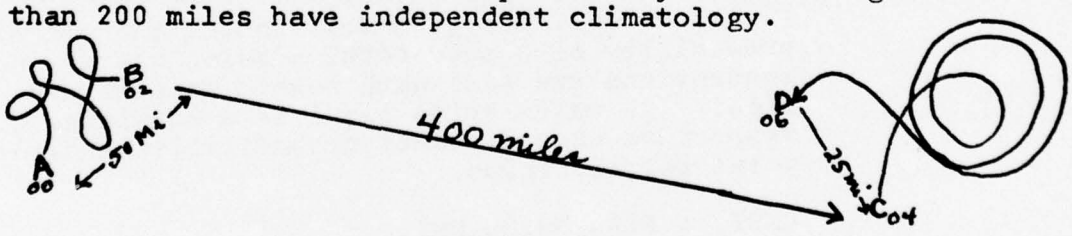

Now A and B are independent of C and D. But A and B are dependent and C and D are dependent. Then, from (2) and (4):

$$CMSI_t = P(A \wedge B \wedge C \wedge D) = P\,[(A \wedge B) \wedge (C \wedge D)] = P(A \wedge B) \text{ times } P(C \wedge D). \quad (5)$$

From (3), $P(A_{\wedge}B) = P(A) + P(B) - P(AUB)$ (6)

But P(AUB) is the probability that at least one of A or B is up. It is readily seen in Fig. 1 that P(AUB) must be larger than either of the two unconditional probabilities and that $P(A_{\wedge}B)$ must be smaller than either of the unconditionals if the two are dependent but not co-located. In accordance with the above, let us arbitrarily assume P(AUB) = .90 as a value reasonably in excess of P(A) and P(B) for the first part of the leg and P(CUD) = .78 as one meeting similar criterion for the latter portion of a flight.

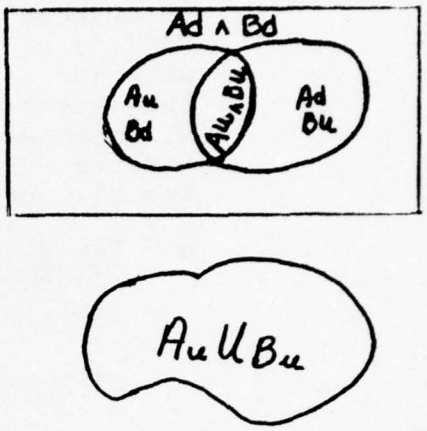

Fig. 1. Intersection and Union.

From (6) $P(A_{\wedge}B) = .85 + 80 - .90 = .75.$

$P(C_{\wedge}D) = .67 + .72 - .78 = .61.$

From (5) $CMSI_t = P(A_{\wedge}B) \times P(C_{\wedge}D) = 75 \times .61 =$

$.458 = 45.8\%.$

This is an increase of 13% over the $CMSI_i$ found in example I. Increasing the number of stations involved would further magnify the difference between $CMSI_i$ and $CMSI_t$ — especially if the stations were sufficiently close together so that their joint climatologies assume relationships in excess of random occurrences.

The above two arbitrary examples serve to illustrate the important point that whenever stations are located sufficiently close together to exhibit dependently related climatologies, the assumption of independence leads to $CMSI_i$'s that are sufficiently pessimistic to be misleading to a decisionmaker

3) $CMSI_t$ Modelling Efforts

Our research efforts have been restricted to modelling relationships of joint probabilities between two different stations with respect to specified visibility and ceiling limitations. A data base was

acquired from ETAC/AWS which contained the computer processed data necessary for these modelling efforts for 39 sets of three-station combinations distributed throughout the Northern Hemisphere. Computer-traced $CMSI_t$'s were computed from these data and tabulated with the respective unconditional probability values. The latter were used to calculate $CMSI_i$ estimates. Differences between $CMSI_t$ and $CMSI_i$ provide a direct measure of the joint dependencies between the two respective stations.

a) The K-factor was proposed to measure this dependency. Its numerical value when multiplied by $CMSI_i$ yields the true CMSI:

$$CMSI_t = CMSI_i \times K = P(Au) \times P(Bu) \times K \qquad (7)$$
$$= \left[1 - P(Ad)\right] \times \left[1 - P(Bd)\right] \times K.$$

Or, solving for K,

$$K = \frac{CMSI_t}{\left[1 - P(Ad)\right] \times \left[1 - P(Bd)\right]}. \qquad (8)$$

It was initially anticipated that the direction of flight from A to B would have a significant bearing on the magnitude of K. To verify this, A was taken as the origin (center) in Fig. 2. The direction and distance to B was aligned with respect to that point and the K-factor was plotted and analyzed. The analysis showed some northeast-southwest elongation as the K-factor approaches 1.000 (independence). However, as the distance decreases, the isolines become almost circular. This led to the conclusion that the climatic joint-dependencies are virtually independent of direction. At very close range, $CMSI_t$ was found to be quite sensitive to errors in the K-factor. Insights gained from a study of the K-factor fields led to the development of other more promising concepts.

b) The M-Factor. The data base was stratified into winter and summer seasons, and distance groups of 0-50, 50-100, 100-200, and 200-300 miles. CMSI's were plotted on the abscissa and $CMSI_t$'s on the ordinate of a graph. Their intersections were noted by dots. A fairly good linear alignment of the dots emerged within each distance range (see Fig. 3). The dots were oriented close to the $CMSI_i$ line for those stations which were very far apart and nearly independent. The more the stations' data were correlated, the closer the dots became oriented to the "perfectly-correlated" line.

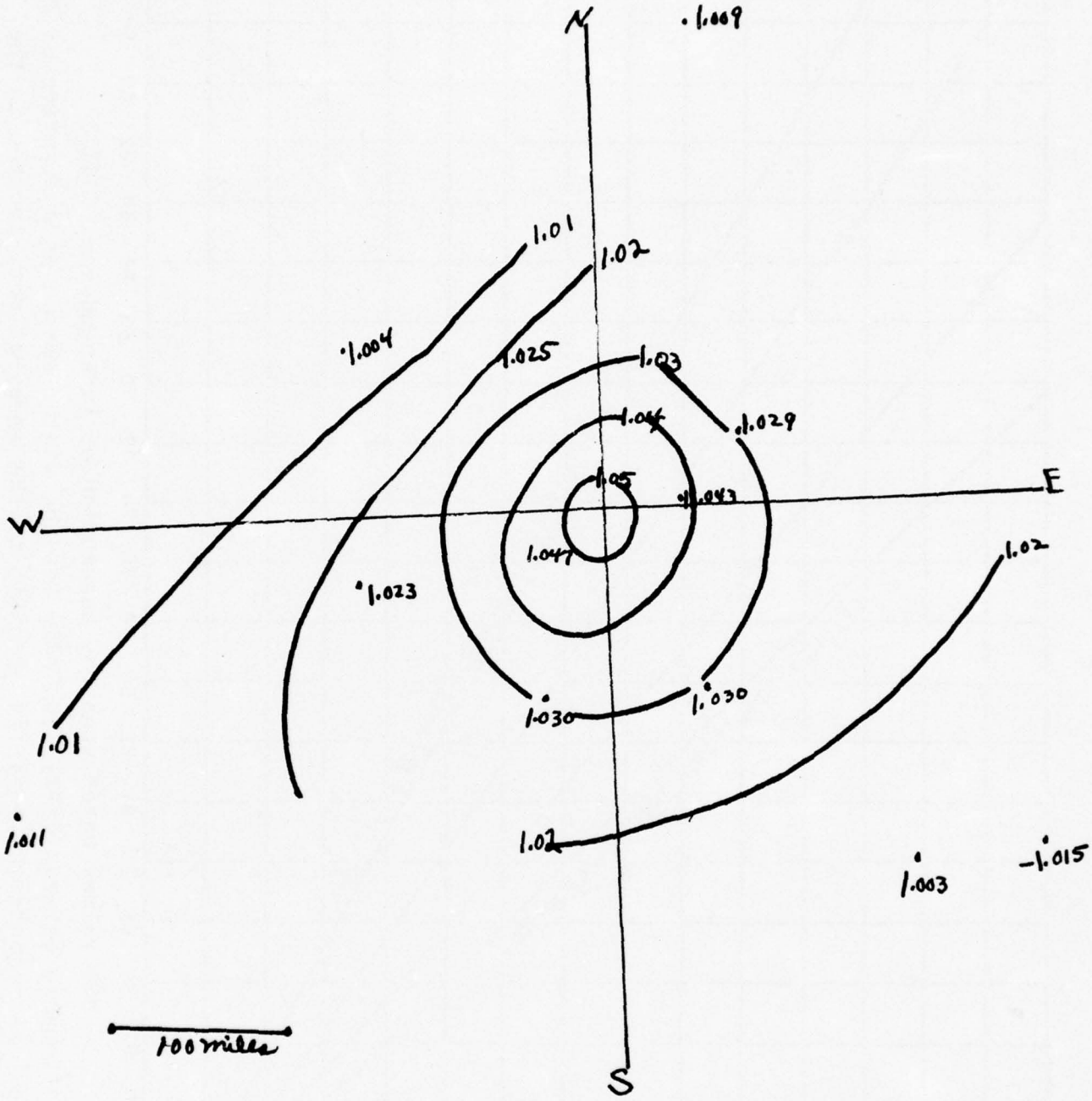

Fig. 2. K-factors for 0000 Local Time in January

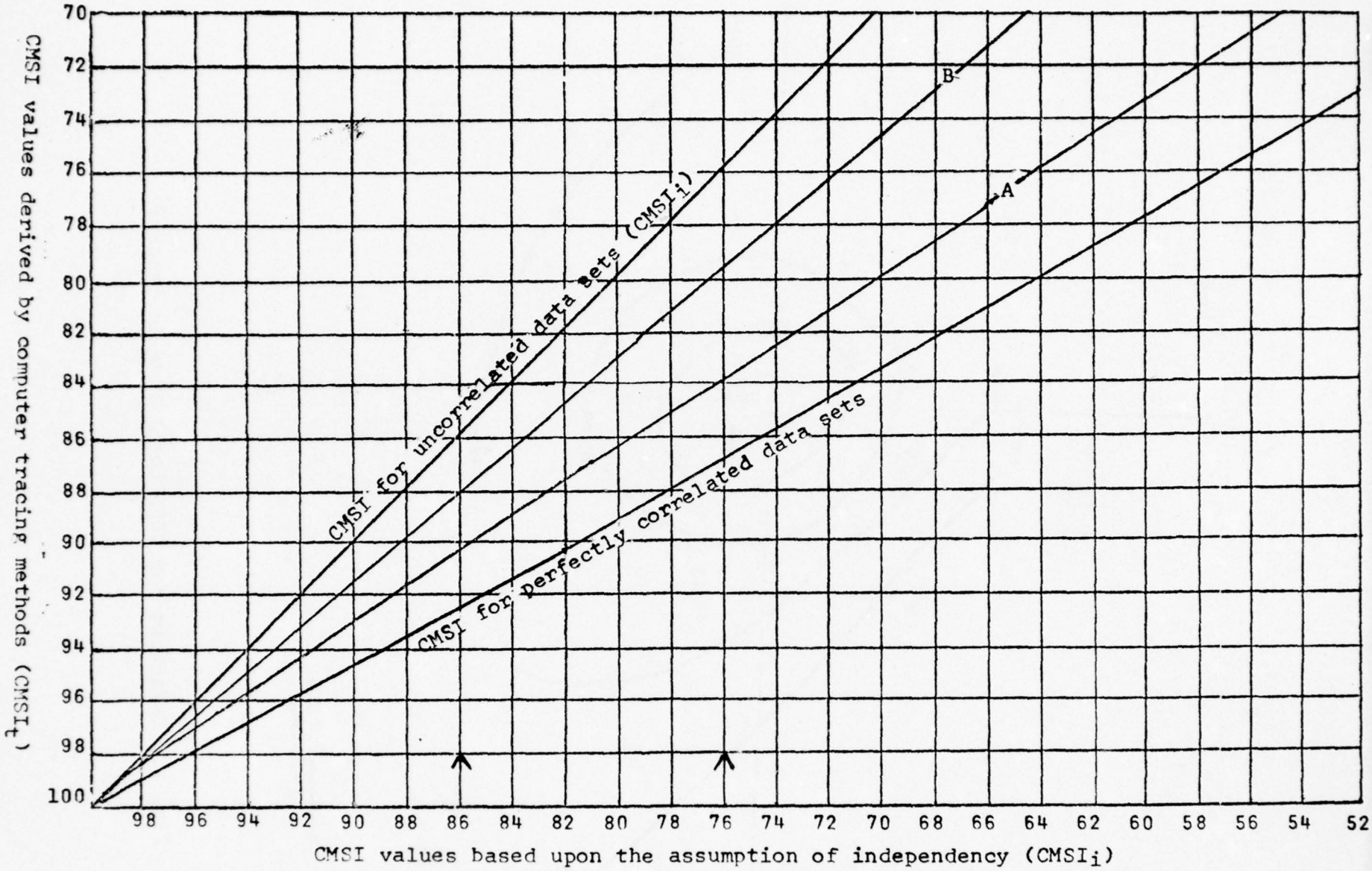

Fig. 3. Relationship between $CMSI_t$ and $CMSI_i$ for the winter season as a function of distance.
Line A represents the best fit of $CMSI_t$ to the array of dots located in the 0-50 mile range.
Line B represents the best fit of $CMSI_t$ to the array of dots located in the 50-100 mile range.

The limits of the slope of the linear relation were confined between the perfectly correlated and uncorrelated representations. Plots of the 500/1 data and those of the 200/½ data were compared. Similar orientations were found with respect to the best-fit lines connecting the respective arrays of dots. The significance of this finding is that a common M-value can be used for the 1000/1 and 500/½ criteria. Presumably this commonality would pertain to other ceiling/visibility categories as well.

The M-factor was defined as follows:

$$CMSI_t = CMSI_i + (1 - CMSI_i) \times M. \qquad (9)$$

Solving for M,

$$M = \frac{CMSI_t - CMSI_i}{1 - CMSI_i} . \qquad (10)$$

Fields of M-factor for 500/1 and 200/½ were generated for all months, for distances from 0 to 250 miles (see Fig. 4). The fields were smoothed in both time and space dimensions. They can be easily analyzed and are consistent with meteorological reasoning in that the M-factor decreases with distance, so that $CMSI_t \rightarrow CMSI_i$. The annual variation is cyclic allowing a smooth transition from month to month.

c) The Alpha Factor. The alpha-factor method was a natural outgrowth of the K- and M-factor research. The data base was again stratified into summer/winter seasons, and mileage ranges of 0-50, 50-100, 100-200, and 200-300. An annual (all months) category for each mileage range was also included. P(Au) = 1 - P(Ad) was put on the ordinate and P(Bu) = 1 - P(Bd) on the abscissa. $CMSI_t$ values were plotted at the intersection of the respective sets of unconditional probabilities (see Figs. 5a, 5b, 5c and 5d).

The smoothed $CMSI_t$ fields were easily analyzed and limits of the isolines were established. The isoline could be no closer to the origin than the solid quasi-diagonal line connecting the two unconditionals (the isoline of independence) and could be no further away from the origin than the square region outlined by the axes and the vertical and horizontal lines of two equal conditionals. The distance on a radial from the origin between the $CMSI_i$ diagonal and the $CMSI_t$ curve is a measure of the

Route Distance in Air Miles

Month	0	10	20	30	40	50	60	70	80	90	100	110	120	130	140	150	160	170	180	190	200	210	220	230	240	250
Jan.	.40	.35	.33	.30	.27	.25	.24	.22	.20	.18	.17	.15	.14	.13	.13	.13	.12	.11	.10	.09	.08	.07	.06	.05	.03	.02
Feb.	.40	.35	.32	.29	.26	.24	.22	.20	.18	.17	.16	.15	.13	.12	.12	.11	.10	.09	.08	.06	.05	.05	.04	.02	.02	.01
March	.40	.34	.31	.28	.25	.23	.21	.19	.17	.15	.13	.12	.10	.09	.08	.06	.05	.04	.03	.02	.00	.00	.00	.00	.00	.00
April	.40	.33	.30	.26	.25	.21	.19	.17	.14	.13	.12	.10	.07	.05	.02	.01	.00	.00	.00	.00	.00	.00	.00	.00	.00	.00
May	.40	.32	.27	.24	.22	.20	.17	.15	.12	.08	.05	.04	.03	.02	.00	.00	.00	.00	.00	.00	.00	.00	.00	.00	.00	.00
June	.40	.31	.26	.22	.20	.17	.15	.12	.10	.07	.04	.03	.02	.01	.00	.00	.00	.00	.00	.00	.00	.00	.00	.00	.00	.00
July	.40	.32	.26	.22	.18	.15	.12	.10	.07	.05	.04	.03	.02	.01	.00	.00	.00	.00	.00	.00	.00	.00	.00	.00	.00	.00
August	.40	.33	.27	.23	.19	.17	.15	.12	.08	.06	.05	.03	.03	.02	.00	.00	.00	.00	.00	.00	.00	.00	.00	.00	.00	.00
Sept.	.40	.33	.31	.26	.21	.18	.16	.15	.11	.10	.07	.06	.05	.04	.03	.02	.01	.00	.00	.00	.00	.00	.00	.00	.00	.00
Oct.	.40	.34	.32	.28	.26	.22	.18	.16	.15	.13	.12	.11	.10	.09	.08	.06	.05	.04	.03	.02	.02	.00	.00	.00	.00	.00
Nov.	.40	.34	.33	.31	.27	.25	.22	.19	.17	.16	.15	.14	.13	.11	.10	.09	.08	.07	.06	.05	.04	.04	.03	.02	.00	.00
Dec.	.40	.35	.34	.31	.28	.25	.23	.22	.20	.19	.18	.17	.15	.15	.14	.13	.13	.12	.11	.10	.08	.06	.05	.04	.03	.02

M-factors for expressing meteorological homogeneity for ceiling conditions less than 500' and/or visibilities less than one mile as a function of distance and month.

Route Distance in Air Miles

Month	0	10	20	30	40	50	60	70	80	90	100	110	120	130	140	150	160	170	180	190	200	210	220	230	240	250
Jan.	.40	.35	.31	.28	.25	.21	.20	.17	.16	.15	.13	.12	.11	.10	.08	.07	.07	.07	.06	.05	.04	.03	.02	.01	.00	.00
Feb.	.40	.35	.31	.27	.24	.20	.18	.17	.15	.14	.12	.11	.10	.09	.07	.07	.05	.05	.03	.02	.01	.01	.00	.00	.00	.00
March	.40	.34	.30	.26	.22	.19	.16	.14	.12	.10	.09	.08	.07	.05	.04	.03	.01	.01	.00	.00	.00	.00	.00	.00	.00	.00
April	.40	.34	.30	.25	.21	.17	.14	.11	.10	.08	.06	.05	.03	.02	.01	.01	.00	.00	.00	.00	.00	.00	.00	.00	.00	.00
May	.40	.34	.30	.25	.20	.17	.13	.10	.08	.05	.03	.02	.00	.00	.00	.00	.00	.00	.00	.00	.00	.00	.00	.00	.00	.00
June	.40	.34	.30	.24	.19	.16	.12	.09	.06	.04	.02	.01	.00	.00	.00	.00	.00	.00	.00	.00	.00	.00	.00	.00	.00	.00
July	.40	.34	.30	.24	.19	.16	.12	.09	.07	.03	.00	.00	.00	.00	.00	.00	.00	.00	.00	.00	.00	.00	.00	.00	.00	.00
August	.40	.34	.30	.25	.20	.17	.14	.11	.08	.05	.02	.01	.00	.00	.00	.00	.00	.00	.00	.00	.00	.00	.00	.00	.00	.00
Sept.	.40	.35	.31	.26	.21	.18	.15	.13	.10	.09	.06	.03	.02	.00	.00	.00	.00	.00	.00	.00	.00	.00	.00	.00	.00	.00
Oct.	.40	.35	.31	.27	.22	.19	.17	.14	.12	.10	.08	.05	.04	.03	.02	.00	.00	.00	.00	.00	.00	.00	.00	.00	.00	.00
Nov.	.40	.35	.32	.28	.23	.20	.17	.15	.14	.12	.10	.08	.06	.05	.04	.04	.02	.01	.00	.00	.00	.00	.00	.00	.00	.00
Dec.	.40	.35	.32	.28	.25	.21	.18	.16	.15	.14	.12	.10	.08	.07	.06	.05	.04	.03	.03	.02	.02	.01	.00	.00	.00	.00

Fig. 4. M-Factors for expressing meteorological homogeneity for ceiling conditions less than 200' and/or visibilities less than 1/2 mile as a function of distance and month.

To obtain estimated MSI values for given route distances

1) Calculate the MSI value given by the assumption of independency, i.e., $(1-P_D)(1-P_A)$ where P_D is the unconditional probability at take-off and P_A is the unconditional probability one hour later at the arrival station.

2) Add to that value the product of one minus the independency calculation of step 1 times the appropriate M-factor.

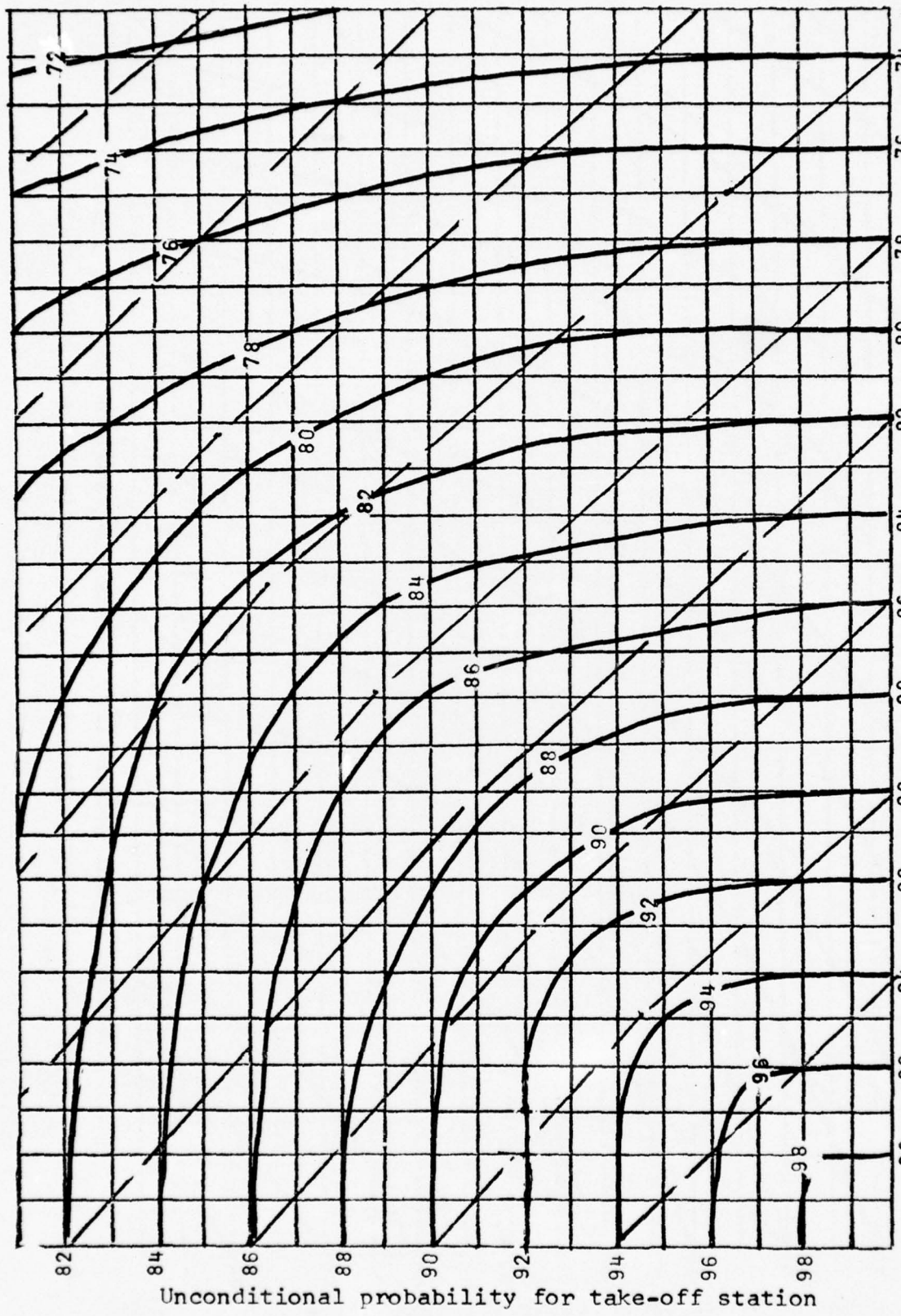

Fig. 5a. Graph of CMSIt (heavy curved lines) for Lakenheath-Mildenhall and Mildenhall-Lakenheath comprising the distance interval of 0-50 miles for all months of the year. The dashed lines pertain to CMSIi. The numbers along the co-ordinate axis pertain to either set of CMSI values.

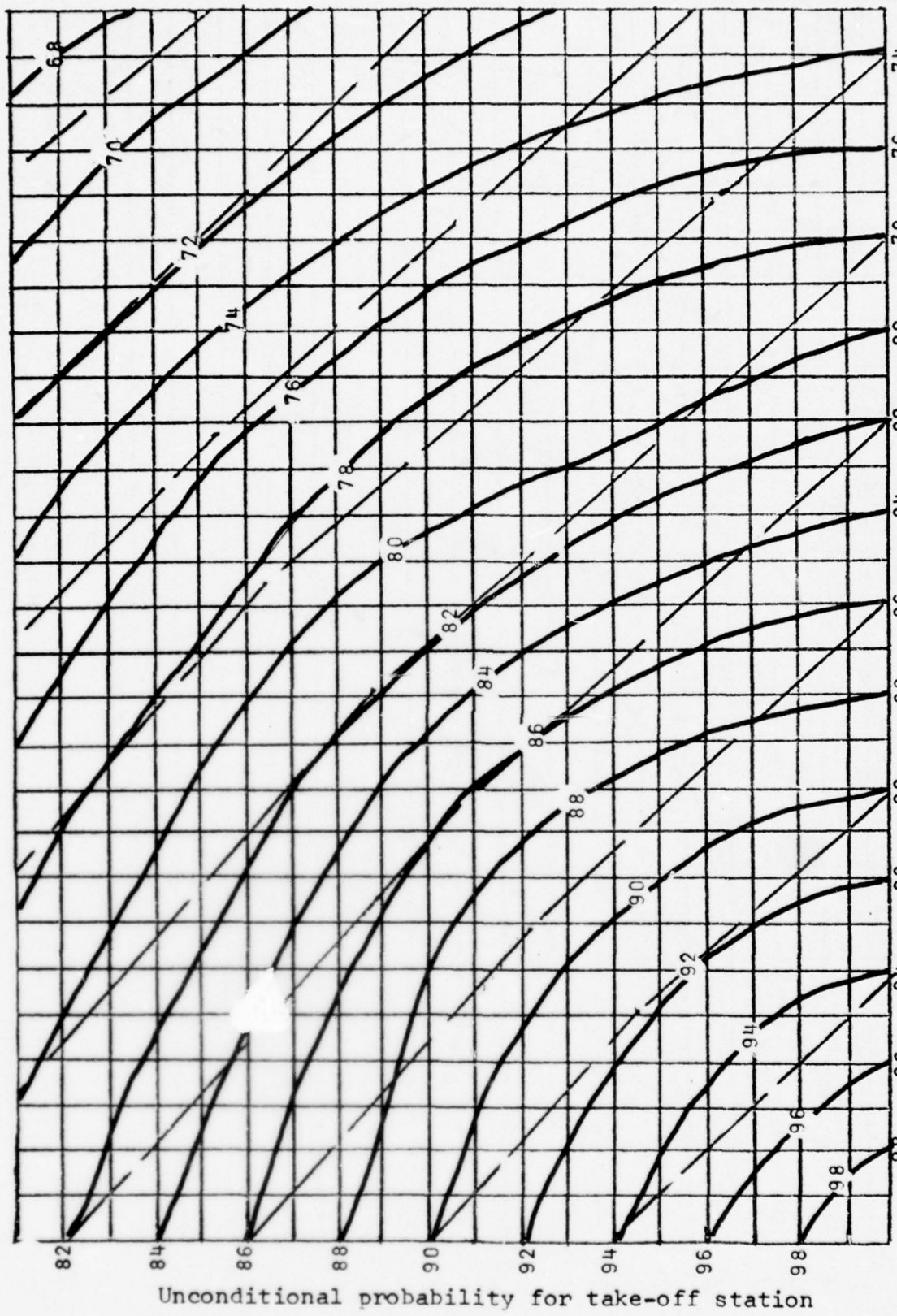

Fig. 5b. Graph of CMSIt (heavy curved lines) for Ramstein-Rhein Main, Rhein Main-Ramstein, Dover-McGuire, McGuire-Dover and Andrews-Dover comprising the distance interval of 50-100 miles for all months of the year. The dashed lines pertain to CMSIi. The numbers along the coordinate axis pertain to either set of CMSI values.

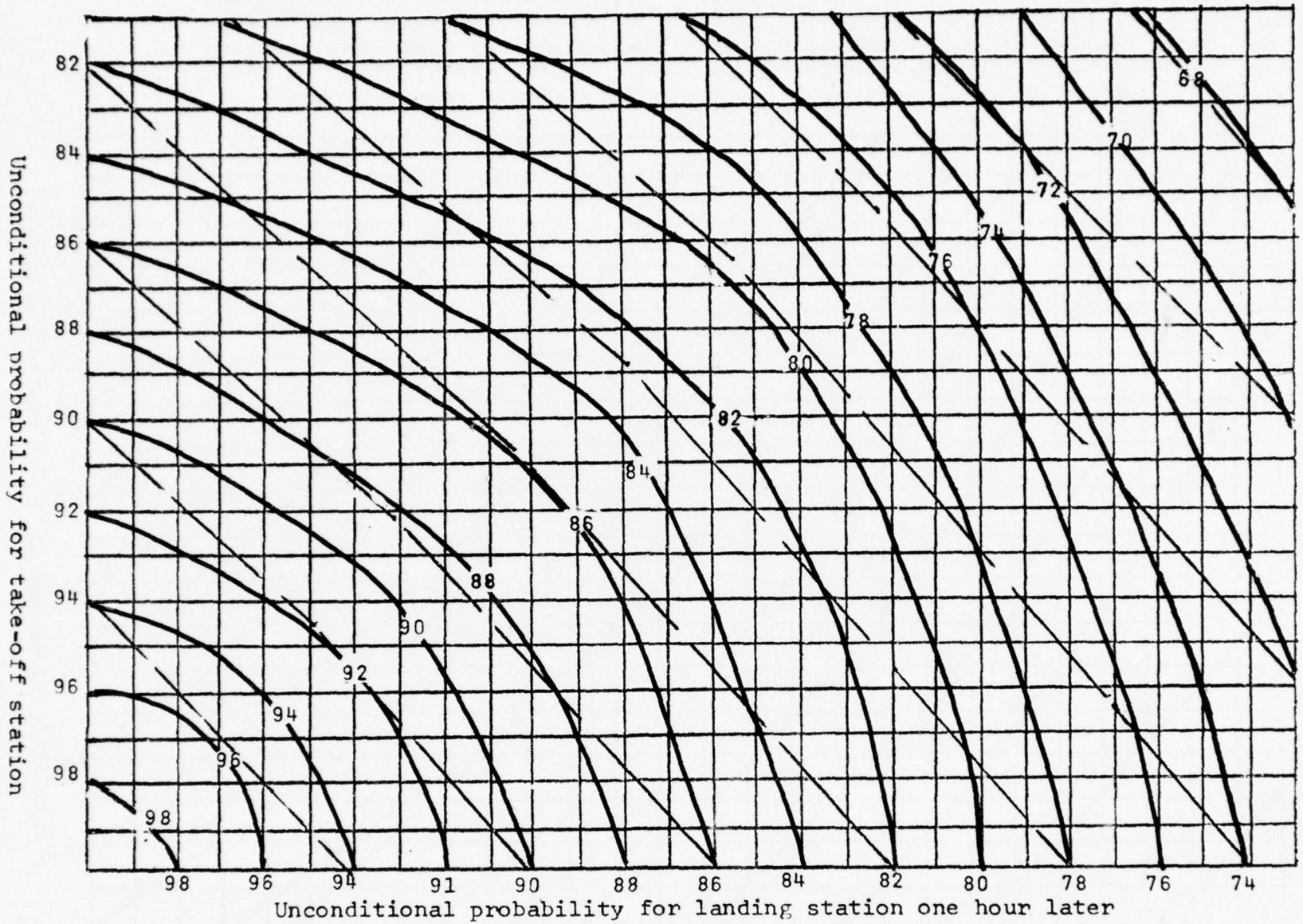

Fig. 5c. Graph of $CMSI_t$ (heavy curved lines) for Pope-Charleston, S.C., Charleston-Robins, Robins-Dobbins, Benning-Robins, Ft. Hood-Bergstrom, Altus-Tinker, and Dobbins-Robins comprising the distance interval of 100-200 miles for all months of the year. The dashed lines pertain to $CMSI_j$. The numbers along the coordinate axis pertain to either set of CMSI values.

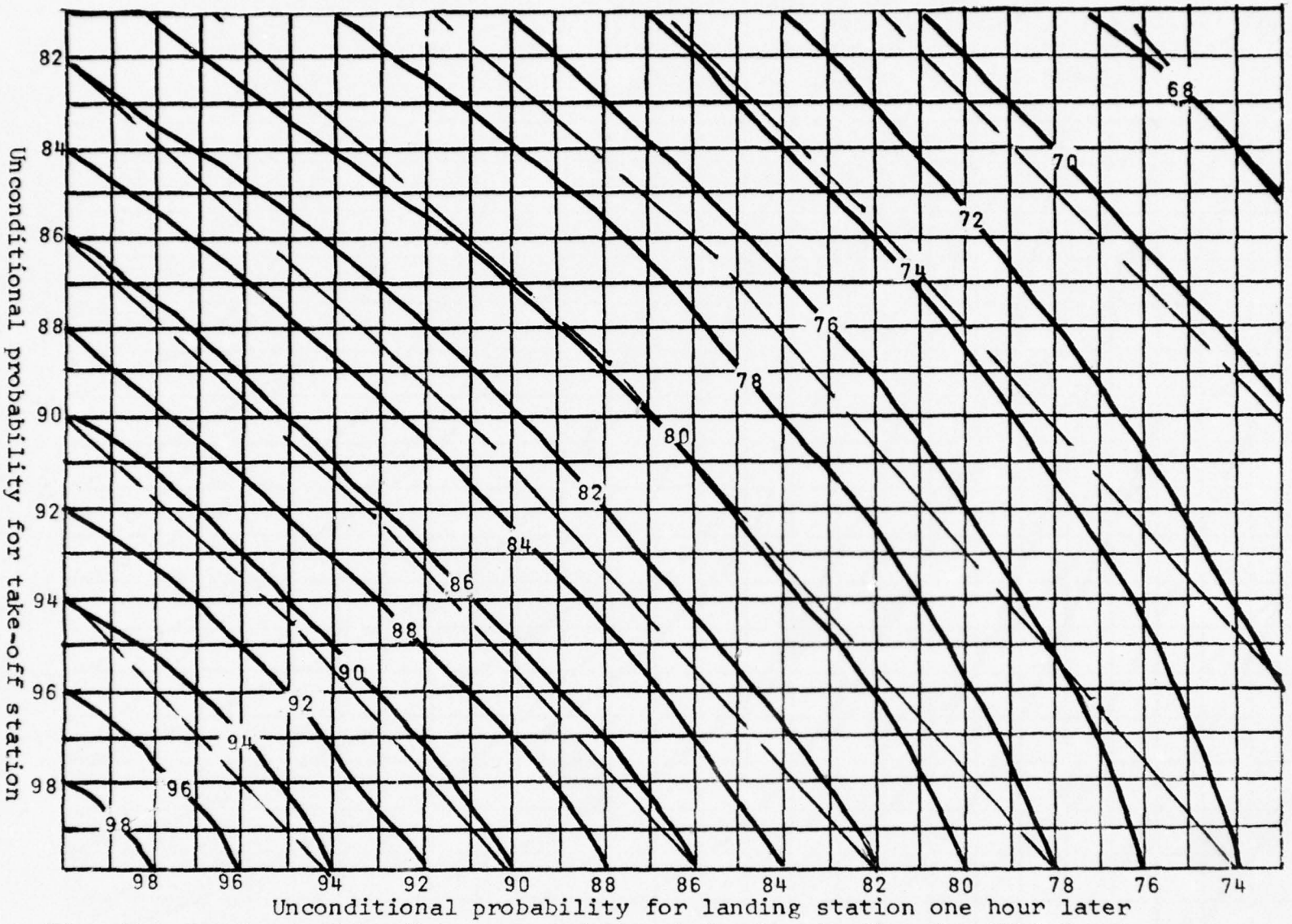

Fig. 5d. Graph of $CMSI_t$ (heavy curved lines) for Travis-Alameda, Hill-Mt. Home, Eielson-Elmendorf, Rota-Torrejon, Moron-Torrejon and Torrejon-Moron comprising the distance interval of 200-300 miles for all months of the year. The dashed lines pertain to $CMSI_i$. The numbers along the coordinate axis pertain to either set of CMSI values.

increase of $CMSI_t$ over $CMSI_i$ due to the dependent relationship between stations. Note that the curvature of the isolines decreases with increasing distance so that $CMSI_t \rightarrow CMSI_i$. The quantitative measure of this curvature change is also a measure of the change of dependence. CMSI-graphs for both 500/1 and 200/½ were produced to learn (as was the case for the M-factor values) that a common graph would suffice for both sets of ceiling/visibility criteria.

i) An analytic function was developed to capture the relationships contained in these graphs. To do this, the $CMSI_t$ field was set up on an X, Y cartesian coordinate system with X = P(Bd) = 1 - P(Bu), and Y = P(Ad) = 1 - P(Au) (see Fig. 6). The field was assumed to be symmetric about

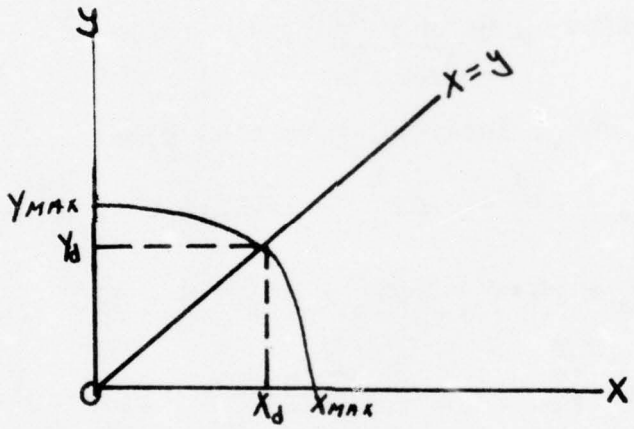

Fig. 6. Schematic representation of the Alpha-factor.

the diagonal (x = y). A hyperbolic function which describes a curve similar to the $CMSI_t$ isoline is

$$(X - G)(Y - G) = H^2 \qquad (11)$$

where G and H are constants on a given isoline.

At X = 0.0, $Y = Y_{maximum} = Y_m$

so, $(0 - G)(Y_m - G) = H^2$, or

$$H^2 = G^2 - G\,Y_m \,. \qquad (12)$$

On the diagonal, $X = X_d = Y_d = Y$, so

$$(X_d - G)(Y_d - G) = (Y_d - G)(Y_d - G) = (Y_d - G)^2 = H^2 \qquad (13)$$

Combining (12) and (13)

$$H^2 = G^2 - GY_m = (Y_d - G)^2. \qquad (14)$$

The numerical value of the $CMSI_t$ isoline is the CMSI value desired. It is also the value of $(1 - Y_m)$ on the same isoline. At any point in the first quadrant the Y_m value of the isoline which passes through it defines $CMSI_t$. Assuming "concentric" or equal spacing between isolines of $CMSI_t$, the ratio Y_d/Y_m is a constant for a given graph within a given distance range.

We shall define $\alpha \equiv \frac{Y_d}{Y_m} = \frac{X_d}{X_m}$. (15)

Then, $Y_d = \alpha Y_m$, inserted into (14) gives

$$(\alpha Y_m - G)^2 = \alpha^2 Y_m^2 - 2\alpha G Y_m + G^2 = G^2 - GY_m .$$

$$\alpha^2 Y_m^2 = 2G\alpha Y_m - GY_m = GY_m(2\alpha - 1). \qquad (16)$$

$$G = \frac{\alpha^2 Y_m^2}{Y_m(2\alpha - 1)} = \frac{\alpha^2 Y_m}{2\alpha - 1} .$$

From (13), (15), and (16)

$$H^2 = (Y_d - G)^2 = (\alpha Y_m - \frac{\alpha^2 Y_m}{2\alpha - 1})^2 .$$

$$H = \alpha Y_m - \frac{\alpha^2 Y_m}{2\alpha - 1} = \frac{2\alpha^2 Y_m - \alpha Y_m - \alpha^2 Y_m}{2\alpha - 1} = \qquad (17)$$

$$\frac{\alpha^2 Y_m - \alpha Y_m}{2\alpha - 1} = \frac{\alpha Y_m (\alpha - 1)}{2\alpha - 1} .$$

Putting H and G from (16) and (17) back into the original function (11),

$$(X - G)(Y - G) = H^2, \text{ gives}$$

$$\left(X - \frac{\alpha^2 Y_m}{2\alpha - 1}\right)\left(Y - \frac{\alpha^2 Y_m}{2\alpha - 1}\right) = \left(\frac{\alpha Y_m(\alpha - 1)}{2\alpha - 1}\right)^2 .$$

$$XY - X\left(\frac{\alpha^2 Y_m}{2\alpha - 1}\right) - Y\left(\frac{\alpha^2 Y_m}{2\alpha - 1}\right) + \left(\frac{\alpha^2 Y_m}{2\alpha - 1}\right)^2 = \frac{\alpha^2 Y_m^2(\alpha - 1)^2}{(2\alpha - 1)^2} .$$

$$XY - \left(\frac{\alpha^2 Y_m}{2\alpha - 1}\right)(X + Y) + \frac{\alpha^4 Y_m^2}{(2\alpha - 1)^2} - \frac{\alpha^2 Y_m^2 (\alpha - 1)^2}{(2\alpha - 1)^2} = 0 .$$

This can be written as a polynomial in Y_m and solved by the quadratic formula

$$Y_m^2\left(\frac{\alpha^4 - \alpha^2(\alpha^2 - 2\alpha + 1)}{(2\alpha - 1)^2}\right) + Y_m\left(\frac{-\alpha^2(X + Y)}{2\alpha - 1}\right) + XY = 0 .$$

$$Y_m^2\left(\frac{\alpha^4 - \alpha^4 + 2\alpha^3 - \alpha^2}{(2\alpha - 1)^2}\right) + Y_m\left(\frac{-\alpha^2(X + Y)}{(2\alpha - 1}\right) + XY = 0 .$$

$$Y_m^2\left(\frac{\alpha^2(2\alpha - 1)}{(2\alpha - 1)^2}\right) + Y_m\left(\frac{-\alpha^2(X + Y)}{2\alpha - 1}\right) + XY = 0 .$$

$$Y_m^2(\alpha^2) + Y_m(-\alpha^2(X + Y)) + XY(2\alpha - 1) = 0 .$$

$$Y_m = \frac{-(-\alpha^2(X + Y)) \pm \sqrt{(-\alpha^2(X + Y))^2 - 4(\alpha^2)(XY(2\alpha - 1))}}{2(\alpha^2)} .$$

$$Y_m = \frac{\alpha^2(X + Y)}{2\alpha^2} \pm \sqrt{\frac{\alpha^4(X + Y)^2}{4\alpha^4} - \frac{4\alpha^2(XY(2\alpha - 1))}{4\alpha^4}} .$$

$$Y_m = \frac{X + Y}{2} \pm \sqrt{\frac{(X + Y)^2}{4} - XY\frac{(2\alpha - 1)}{\alpha^2}} . \qquad (18)$$

$X = P(Bd)$, $Y = P(Ad)$, $CMSI_t = 1 - Y_m$ and α is a constant value within a given distance range. Applying the positive root from (18) yields

$$CMSI_t = 1 - Y_m = 1 - \frac{P(Ad) + P(Bd)}{2} - \sqrt{\left[\frac{P(Ad) + P(Bd)}{4}\right]^2 - \left(P(Ad)\right)\left(P(Bd)\right)\left(\frac{2\alpha - 1}{\alpha^2}\right)} \qquad (19)$$

A mean α was calculated for each distance range and $CMSI_t$ fields were calculated using (19). Agreement with the original fields was quite good. In summary, given P(Ad), P(Bd), and a table of $\bar{\alpha}$ values, estimated $CMSI_t$ could be generated by analytic formulation.

ii) The next step was to formulate the Alpha-factor as a function of distance and month. Station combinations with similar separation-distances were grouped and $CMSI_t$ graphs were generated for December/January and June/July for a 1-hr lag. The limits of α were known to range from $0.5 < \alpha \leq 1.0$. The function,

$$\alpha = \frac{e^{-s/\gamma} + 1}{2}, \qquad (20)$$

was found to be a fairly good representation of the curve in Fig. 7 when γ is set equal to 70 for Dec/Jan, and 30 for Jun/Jul.

The function, $\gamma = 50 + 20 \cos\left[\frac{(M-1)\pi}{6}\right]$, (21)

was introduced to account for the annual variation of γ.

Here M identifies the month with January = 1 and December = 12 and S represents distance.

iii) The complete Alpha function then, is

$$\gamma = 50 + 20 \cos \left[\frac{(M-1)\pi}{6}\right] .$$

$$\alpha = \frac{e^{-s/\gamma} + 1}{2} .$$

$$CMSI_t = 1 - \frac{P(Ad)+P(Bd)}{2} - \sqrt{\left[\frac{P(Ad)+P(Bd)}{4}\right]^2 - P(Ad)P(Bd)\frac{(2\alpha - 1)}{\alpha^2}} . \quad (22)$$

Equation 22 permits the calculation of $CMSI_t$ from a knowledge of the two unconditional probabilities, the separation distance, and the month. This involves no special graphs. Only trigonometric and exponential tables are needed.

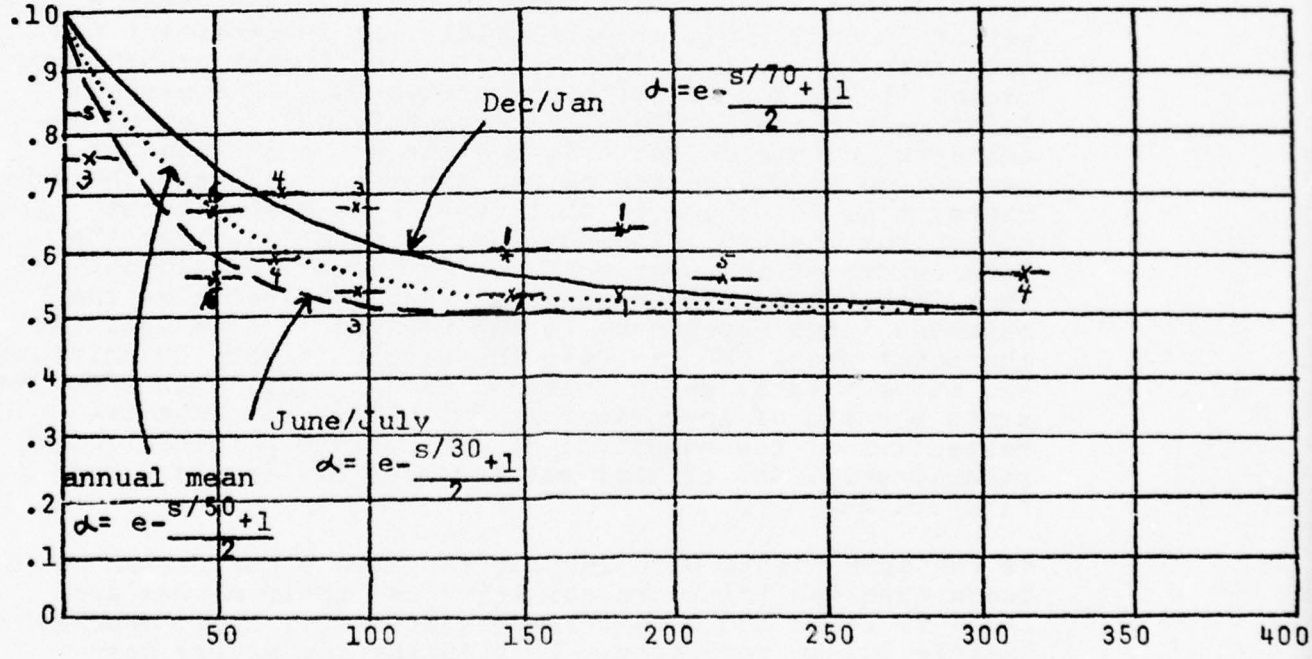

Fig. 7. Values of $\bar{\alpha}$ as a function of distance for winter, summer and the annual mean. The numbers in the drawing refer to the number of stations used in that distance range to produce these values.

d) The Billiken Factor (BF)

The K-factor, M-factor and α -factor method provide ways of modelling joint probability relationships as a function of distance and season. They do, however, have certain shortcomings that can be circumvented. The K-factor and M-factor techniques act to modify the assumption of independency. No attempt is made to distinguish the relative magnitudes of the unconditional probabilities involved. For example, a $CMSI_i$ of 81% could be made up of two unconditional probabilities of 90% each or one of 100% and another of 81%. In the first instance the possibility of a joint relationship of 10% exists. In the latter case the possibility of a joint-relationship is zero. Thus the K-factor and M-factor method work best under certain implied homogeneties of unconditional probability magnitudes. They fail when these conditions are not met.

The α -factor method remedies this situation. It demands, however, that a large number of graphs be constructed. A fifty-mile range is much too large in the proximity of a station to accurately pin down an exponential decay curve. A clue to an alternative solution to the problem is found in figure 3. Here the distance between the perfectly correlated line and the $CMSI_i$ line represents the maximum joint dependency possible between two stations under a given set of unconditional probabilities. It is important to note that the smaller of the two unconditional probability values (1-PA) and (1-PB) also defines this same maximum joint relationship. To illustrate this point, let us examine two points on curve A, one where the independent assumption as designated on the abscissa is 76 and the other where it is 86. We note that curve A is spaced about 4 graph units from the $CMSI_i$ line at the 76% point and that the total width of the sector of maximum joint relationship at that interval is some 5½ units. Hence the ratio of the observed joint dependency to the maximum is some 70%. At the point where CMSI is 86%, the sector is some 3¾ units wide and curve A takes up 2¼ units of that value. This also represents a ratio of approximately 70%. Thus somewhat irrespective of the magnitude of the maximum possible joint relationship, 30% of that value decays off in the first fifty miles.

At the same points with respect to curve B the ratios between observed joint probabilities and their maxima are 1-3/4 to 5-1/2 and 1 to 3-1/4 respectively, i.e., approximately 30% in each case. This factor (or ratio) has come to be called the Billiken factor (BF). It can readily be determined from the data base of each and every station thereby eliminating the problem of constructing voluminous networks of graphs to model the decay of joint dependencies with distance.

The CMSI is the probability that both A and B are up or one minus the probability that either one of A or B is down (i.e., one minus the probability that both will not be up).

$$CMSI_t = P(Au_{\wedge} Bu) = 1 - P\ (AdUBd). \tag{23}$$

From (3),

$$P(AdUBd) = P(Ad) + P(Bd) - P(Ad_{\wedge}Bd). \tag{24}$$

The maximum possible value of the intersection is the smaller of the two unconditional probabilities. Given two unconditional probabilities, they are obviously either equal or one is larger than the other. Let us assume $P(Ad) \geq P(Bd)$ and define L such that

$$L \text{ X } P(Bd) = P(Ad_{\wedge}Bd). \tag{25}$$

Then from (24)

$$P(AdUBd) = P(Ad)+P(Bd) - L \text{ X } P(Bd) = P(Ad)+P(Bd) \text{ X } (1-L)$$

and from (23)

$$CMSI_t = 1 - \left[P(Ad) + (1-L) \text{ X } P(Bd)\right].$$

We shall define the Billiken factor as $BF = 1 - L$. (26)

Then, $CMSI_t = 1 - P(Ad) - BF \text{ X } P(Bd)$

$$= 1-(\text{larger uncond.})-BF \text{ X } (\text{smaller uncond.}). \tag{27}$$

The Billiken factor is defined as that numerical value which, when multiplied by the smaller of the two unconditional probabilities, results in the correct $CMSI_t$ in (27). In other words,

$$BF = \frac{1-(\text{larger unconditional}) - CMSI_t}{(\text{smaller unconditional})}$$

or

$$BF = \frac{P(A_u) - P(A_u \wedge B_u)}{P(B_d)} = \frac{P(A_u \wedge B_d)}{P(B_d)} = P(A_u \mid B_d). \tag{28}$$

It is the conditional probability that A is up, given that B is down. Hence it is to be expected that BF will be zero when the distance between A and B is zero, that BF will tend to the limit $P(A_u)$ as the distance increases and that BF could even approach 1.0 for a negative relationship between A and B.

An analytic function has been fit to the 500/1 field. The 200/½ function would be somewhat similar except for adjustments in the empirical constants needed to fit the data in the lower portion of figure 8 rather than that of the upper part. The major feature of the Billiken factor field is its increasing value with increasing distance and its variation with month. The range of the Billiken factor is from 0 to 1.0 but a Billiken factor value greater than P(Au) becomes erroneous unless the joint probabilities between two stations are negatively correlated— a relationship that the data did not conclusively substantiate.

Mean BF values for Dec/Jan and Jun/Jul from Fig. 8 were plotted against distances (see Fig. 9). These curves can be approximated by the function,

$$BF = 1 - e^{-S/\mu} \tag{29}$$

where μ = 150 for Dec/Jan and μ = 64 for Jun/Jul. Plots of BF isolines at constant mileage against month (see Fig. 10) reveal an annual variation which is not centered about the Dec/Jan - Jun/Jul mean. Instead, the curve is dropped somewhat below this mean having a value of μ = 94 for March, April, September, and October. The maximum amplitude of the BF monthly variation is plotted in Figure 11. The amplitude is bounded by zero at zero distance and tends towards zero at infinite distance. Several statistical distribution functions have these properties (i.e., Poisson, Chi Square, etc.). However the function,

$$Amp_{max} = \frac{A \cdot S}{B \cdot \exp(S/C)} ,$$

was found to be the simplest in form. Its coefficients are: A = 0.352, B = 100, C = 117.6.

Thus, $$Amp_{max} = \frac{0.352\ S}{100\ \exp(S/117.6)} . \tag{30}$$

The cyclic portion of the monthly variation is incorporated by introducing the function,

$$\cos\left[\frac{(M + 5)\,\pi}{6}\right].$$

The complete analytic expression for obtaining Billiken factors then becomes

BF = (mean value) + (max amp)X(cyclic variation)

or

$$BF = (1-e^{-S/94}) + \frac{0.352\ S}{100\ \exp(S/117.6)} X \cos\left[\frac{(M+5)\pi}{6}\right] . \tag{31}$$

Route Distance in Air Miles

Month	0	10	20	30	40	50	60	70	80	90	100	110	120	130	140	150	160	170	180	190	200	210	220	230	240	250	260	270	280	290	300
Jan.	0	10	15	22	28	32	35	40	45	47	50	55	56	57	58	59	60	61	64	68	69	70	72	75	77	80	82	83	84	85	86
Feb.	0	10	17	23	30	35	40	45	46	48	51	55	58	60	61	63	65	70	70	73	75	77	78	80	81	82	82	83	84	85	86
March	0	12	20	26	32	35	40	45	50	55	58	61	65	68	70	72	74	77	80	80	85	85	86	87	88	89	90	90	90	90	90
April	0	15	22	30	32	40	45	50	55	60	61	66	70	75	80	81	84	85	87	90	91	92	94	94	95	96	96	96	96	96	97
May	0	17	28	35	40	45	50	57	60	70	75	80	84	86	87	89	91	92	93	95	95	95	95	95	95	96	96	96	96	97	97
June	0	20	30	38	44	50	55	60	65	72	77	82	85	87	90	92	94	95	95	95	95	95	95	95	95	96	96	96	96	97	97
July	0	17	30	40	47	53	60	65	70	74	77	82	84	87	90	92	95	95	95	95	95	95	95	95	95	96	96	96	96	97	97
August	0	16	28	38	46	52	55	63	68	72	75	79	81	84	85	90	90	91	92	92	94	95	95	95	95	96	96	96	96	97	97
Sept.	0	15	20	30	40	44	52	60	62	68	71	74	77	80	82	84	85	88	90	90	91	93	94	94	95	96	96	96	96	97	97
Oct.	0	14	18	25	31	39	47	50	53	59	60	63	65	68	70	72	75	80	83	85	88	90	90	91	92	93	95	96	96	96	97
Nov.	0	12	15	20	27	31	40	45	48	50	52	55	57	60	65	66	68	70	73	75	80	80	82	85	87	88	89	90	90	90	90
Dec.	0	10	14	19	25	30	36	40	43	46	47	50	51	53	55	58	59	62	63	65	69	71	75	80	82	83	83	84	85	85	86

B-Factors for expressing meteorological homogeneity ceilings less than 500' and/or visibilities less than one mile as a function of distance and month.

Route Distance in Air Miles

Month	0	10	20	30	40	50	60	70	80	90	100	110	120	130	140	150	160	170	180	190	200	210	220	230	240	250	260	270	280	290	300
Jan.	0	10	20	28	32	37	48	49	52	54	57	59	62	64	68	69	70	72	74	75	77	80	81	83	85	87	89	90	91	91	91
Feb.	0	10	20	28	34	40	48	51	53	55	60	61	63	68	70	72	73	75	79	80	83	84	85	87	90	92	93	94	94	94	94
March	0	12	22	30	38	46	51	55	60	64	68	70	71	78	80	82	83	84	85	86	88	90	91	93	94	95	95	95	95	95	95
April	0	12	23	32	42	50	57	63	65	70	74	78	80	85	86	88	89	90	92	94	95	95	95	95	95	95	95	95	95	95	95
May	0	11	24	34	43	52	59	65	70	72	79	82	85	87	90	91	92	93	94	95	95	95	95	95	95	95	95	95	95	95	95
June	0	12	23	35	44	52	60	68	73	78	82	84	88	92	93	94	95	95	95	95	95	95	95	95	95	95	95	95	95	95	95
July	0	12	22	31	42	50	60	65	72	80	84	85	90	92	94	95	95	95	95	95	95	95	95	95	95	95	95	95	95	95	95
August	0	12	21	31	41	49	55	60	68	78	82	85	87	90	92	93	94	94	94	94	94	94	94	94	95	95	95	95	95	95	95
Sept.	0	11	20	31	41	48	52	58	62	70	72	80	83	85	87	88	90	91	92	93	93	93	94	94	94	94	95	95	95	95	95
Oct.	0	11	20	30	40	47	51	55	60	65	70	74	77	80	83	84	85	86	90	91	92	92	93	93	93	93	94	94	94	94	94
Nov.	0	10	18	29	38	44	50	52	55	62	65	67	70	72	75	78	80	82	84	86	90	91	92	93	94	94	95	95	95	95	95
Dec.	0	10	18	25	35	40	48	50	54	58	63	65	67	70	72	74	76	78	80	83	85	87	89	91	92	93	94	94	94	94	94

Fig. 8. B-Factors for expressing meteorological homogeneity ceilings less than 200' and/or visibilities less than 1/2 mile as a function of distance and month.

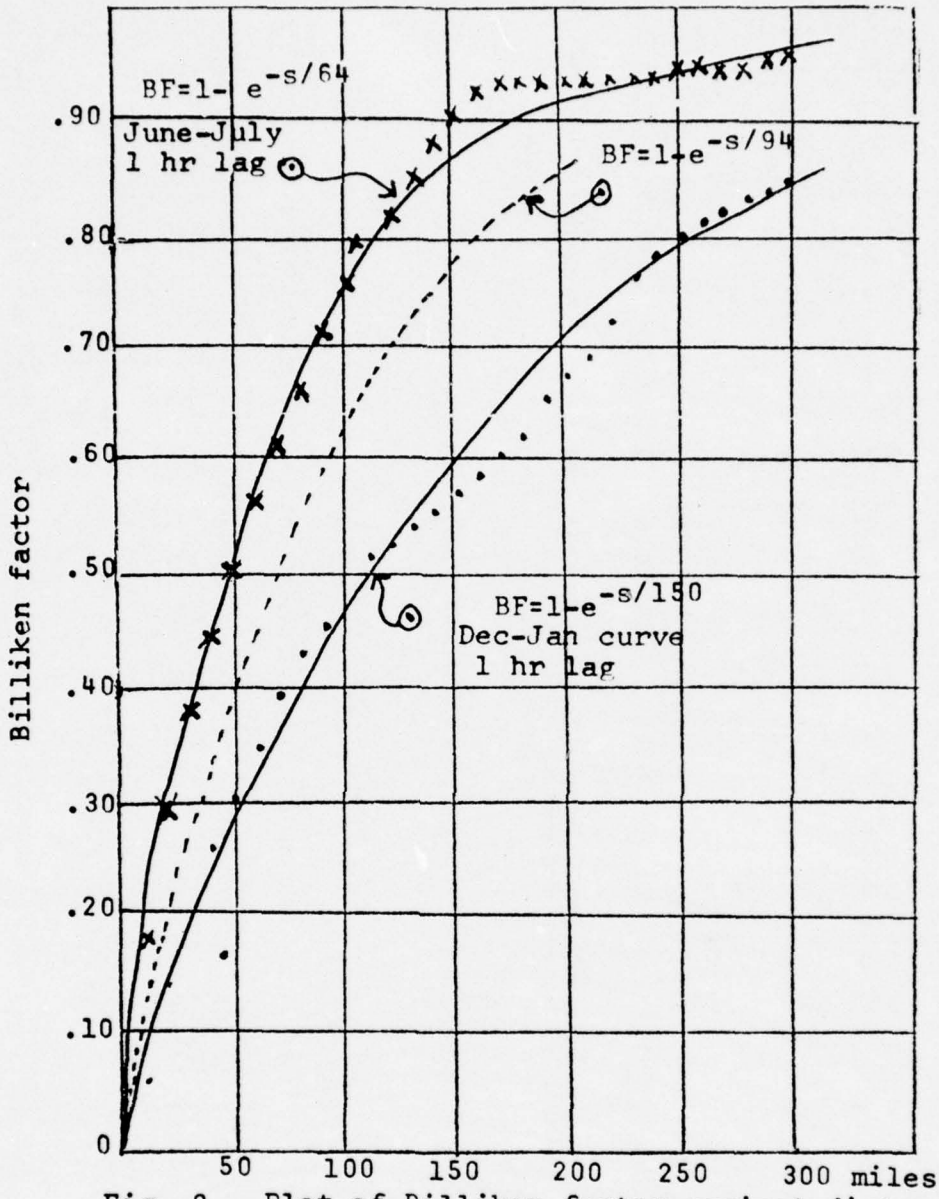

Fig. 9. Plot of Billiken factor against distance for winter, summer and the annual mean. The crosses (x) denote the summer curve obtained from observed data with the adjacent isoline representing the analytic representation for that season. The dotted values next to the Dec.-Jan. curve pertain to the observed trace and the solid line to the analytic formulation for winter.

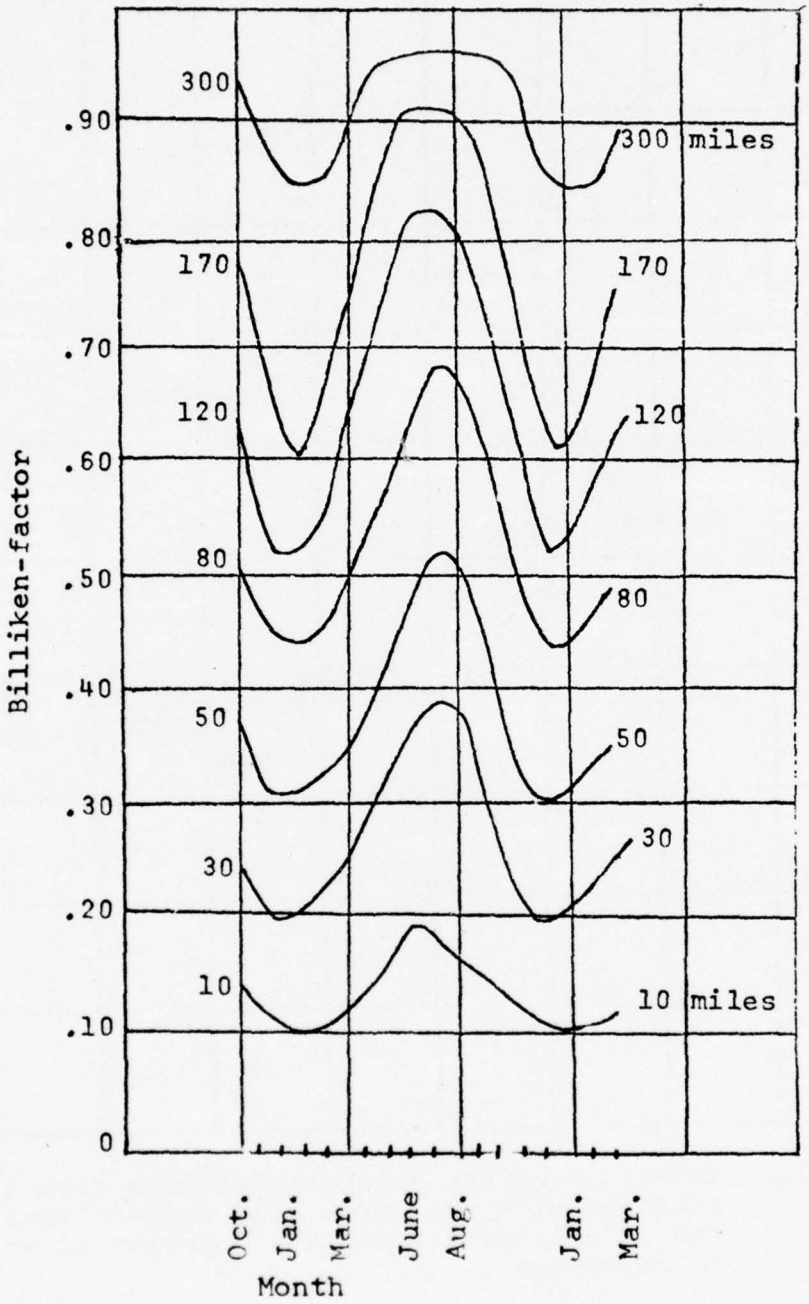

Fig. 10. Billiken-factor isolines for constant mileages plotted against the month of the year.

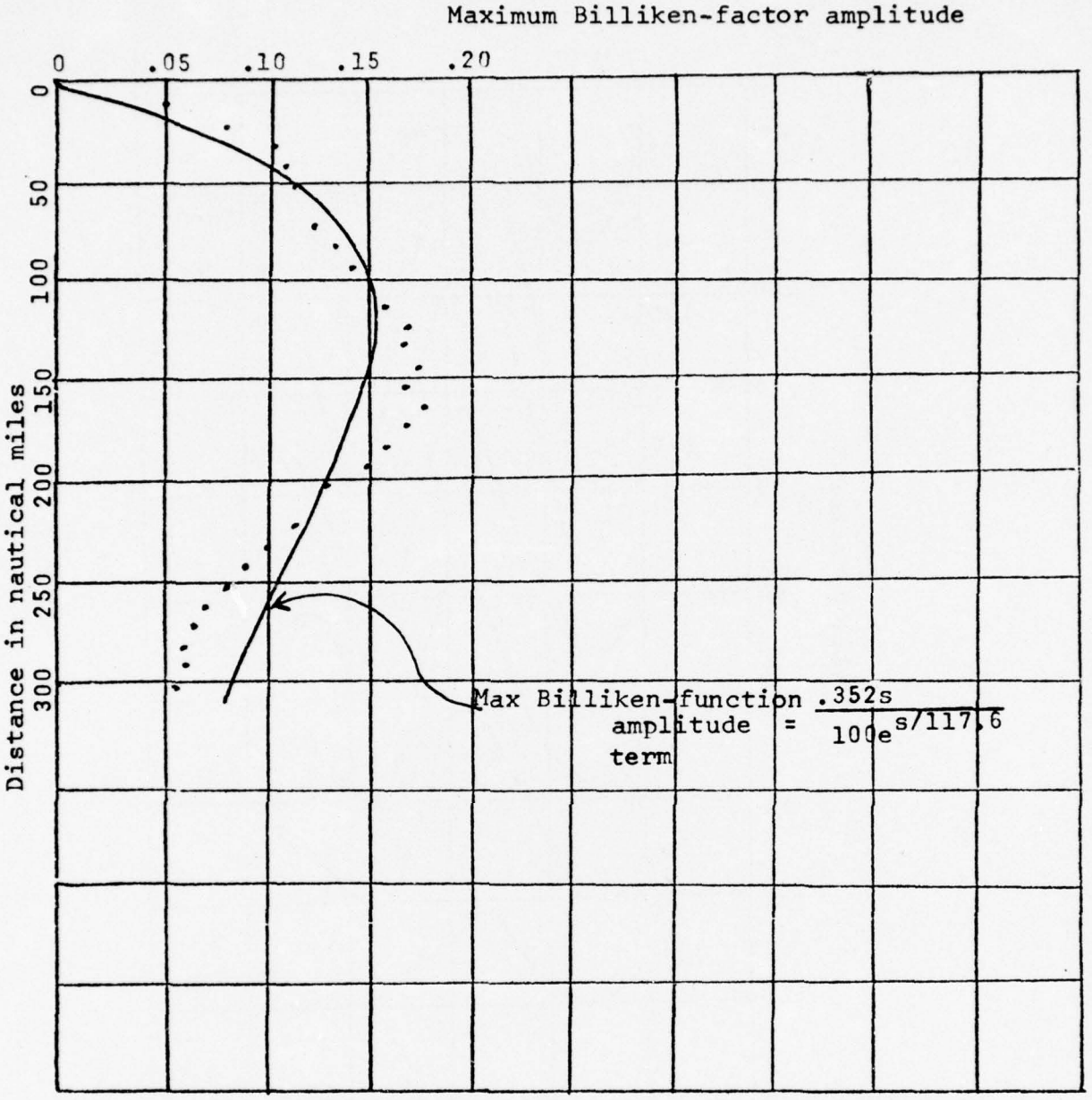

Fig. 11. Variation of the maximum amplitude term of the Billiken function with distance. The dotted lines represent the actual curve which the function is attempting to reproduce.

From (27) the estimated $CMSI_t$ equals 1-(larger uncond) - BF X (smaller uncond).

Equation 31 permits the calculation of $CMSI_t$'s which incorporate seasons and distance dependencies from merely a knowledge of unconditional probabilities and distance and month.

4) **Verifications on Independent Data**

The goals of this verification were to evaluate the three most promising methods of estimating $CMSI_t$ and select the best for further improvements. The first portion of that goal was conducted on independent data only. The improvement phase (second step) incorporated these additional data into the formulae to better tune the coefficient involved. The three methods to be tested were:

1) The Alpha method of equation (22).

2) The graphical Billiken factor of Fig. 8.

3) The analytic formulation of (2) given by equation (3).

The ceiling and visibility criteria of 500 feet/1 mile were chosen with a 1-hour lag time between the various pairs of station combinations with distances ranging from 1 to 306 miles. Data from fifteen different stations were used. Ten locations were in Texas, two in California, and three in the Washington, D. C. area. These data were not used in deriving the analytical functions. January, July and April were selected to provide data representative of the winter, summer and transitional season. The statistics for these months were produced on the Saint Louis University computer using hourly history tapes provided by ETAC. An analysis of these independent data showed the graphical Billiken-factor method to consistently provide the best estimation of the true CMSI. The analytical Billiken-factor method ranked a close second with the Alpha method placing a rather respectable last. Graphical representations of the analytic Alpha and Billiken-factor verifications are shown in figures 12 and 13 for the months of January and April.

The decrease in error-amplitude between January and April is primarily attributable to the better weather conditions (fewer frequencies of low ceilings/visibilities)

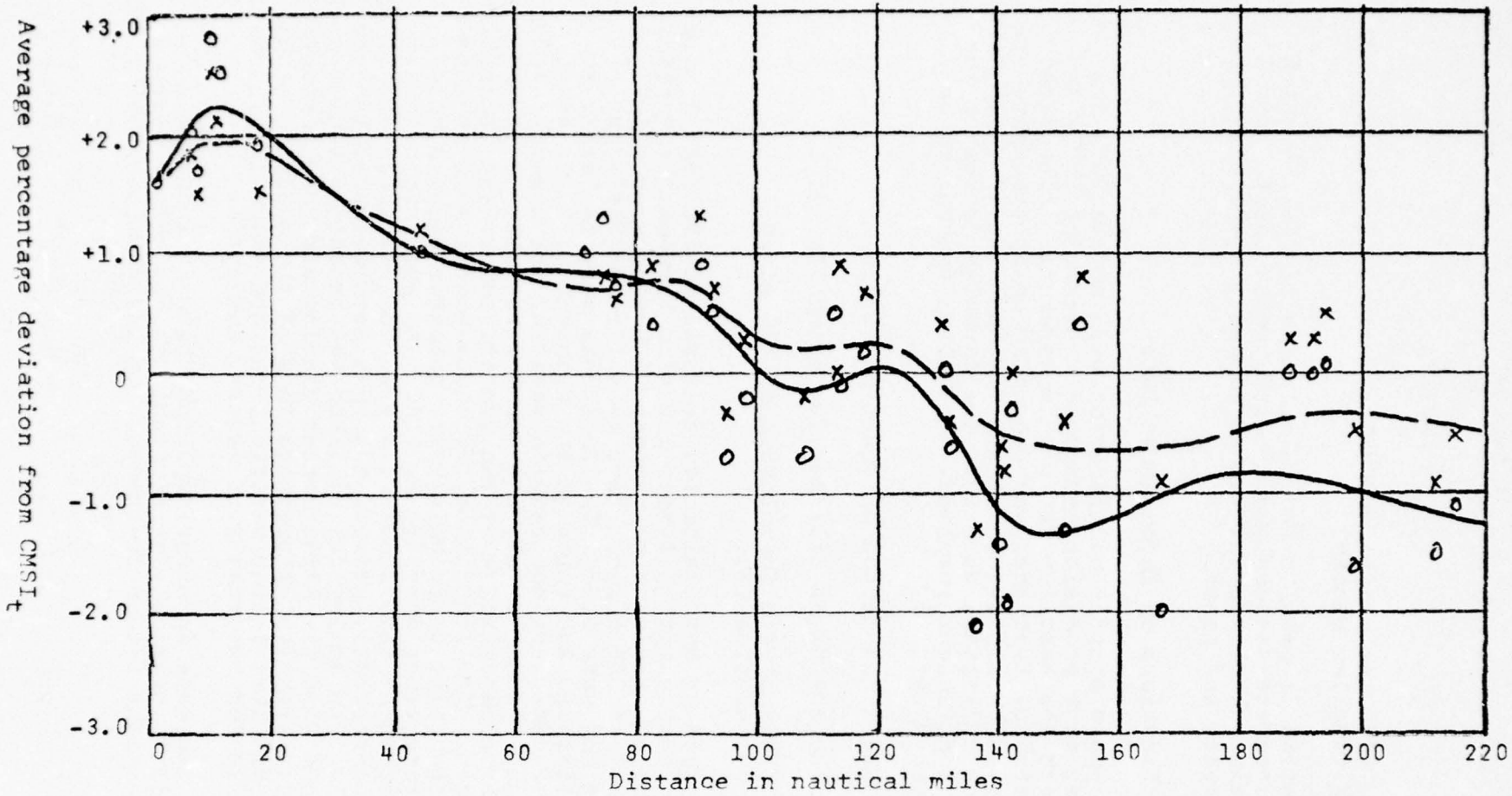

Fig. 12. Relative accuracy of the α-method and BF-method for estimating $CMSI_t$ during the month of Jan.

The small circles and the solid line denote average errors in the α-method. The x's and the dashed line similarily pertain to the analytic BF-method.

The average deviation is defined as $\sum \frac{(CMSI_{(\alpha \text{ or } BF)} - CMSI_t)}{\text{number of readings}}$.

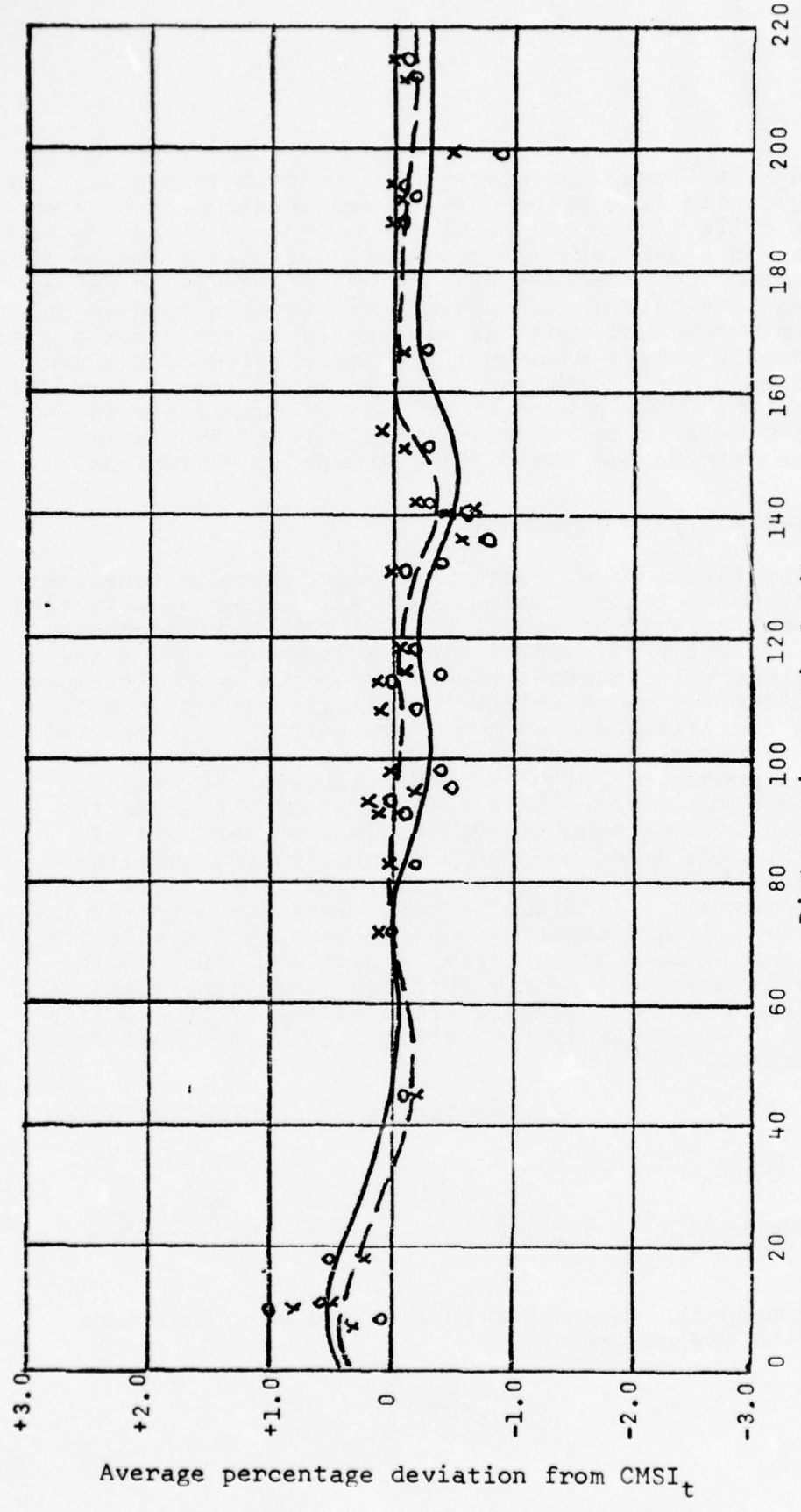

Fig. 13. Relative accuracy of the α-method and BF-method for estimating CMSI$_t$ during the month of April.

The small circles and the solid line denote average errors in the α-method. The x's and the dashed line similarily pertain to the analytic BF-method.

The average deviation is defined as $\Sigma \frac{(\text{CMSI}_{(\alpha \text{ or BF})} - \text{CMSI}_t)}{\text{number of readings}}$.

during the transition months with respect to winter. In fact, during July there were so few occurrences of the 500/1 criteria for the stations tested for either method to show a significant improvement over that given by the assumption of independency. In other words, the $CMSI_t$ estimations best show improvements over the independent assumption method when the weather is at its worse and a dependency exists between the climatologies of the two stations. Verifications of the Billiken-factor method for generating $CMSI_t$'s were first made on completely independent data. Table I gives a summary of the verification results for the fifteen independent stations.

5) **Revised Analytic Functions**

The verifications of Section 4 showed certain consistent biases which could presumably be eliminated by adjusting the coefficients of equation 31. These verifications also exhibit sufficiently close agreement between the graphical Billiken-factor method and its analytic representation for us to select the analytic function method since the latter can be much more readily incorporated into computer oriented procedures. Figure 12 and 13 show a pronounced bias when the distances between stations are short. This is understandable since the coefficients of equation 31, as well as the data of Fig. 8, were based upon only two routes (Lakenheath-Mildenhall and Mildenhall-Lakenheath) in the 0 to 50 mile distance. To minimize this bias, the formerly independent data processed by Saint Louis University for stations located close together were now added to the formerly dependent sample obtained from ETAC to enlarge the data base and permit a finer tuning of the coefficients. Recalling from equation 31, the original formulation was

mean value — max. amplitude — cyclic variation

$$BF = 1 - \exp(-S/94) + \frac{0.352\ S}{100\ \exp(S/117.6)} \times \cos\left(\frac{(m+5)\pi}{6}\right). \quad (31)$$

Based upon the expanded data base the max. amplitude function was changed to

$$\frac{0.0041\ S}{\exp(s/115)}\ .$$

Route	Distance (nm)	Month-January
Washington, D. C. - Bolling AFB	1	100
Bolling AFB - Andrews AFB	7	100
Washington, D. C. - Andrews AFB	8	88
Randolph AFB - San Antonio	10	100
Kelly AFB - San Antonio	11	100
Randolph AFB - Kelly AFB	18	100
Ft. Hood - Waco	45	100
San Francisco - Sacramento	75	100
Ft. Hood - Randolph AFB	95	100
Kelly AFB - Ft. Hood	108	100
San Antonio - Corpus Christi	118	88
Ft. Hood - Dallas	118	100
Reese AFB - Dyess AFB	131	100
Ft. Hood - Dyess AFB	132	100
Randolph AFB - Waco	136	100
San Antonio - Waco	140	100
Dyess AFB - Dallas	154	71
Waco - Victoria	167	100
Dyess - San Antonio	188	50
Randolph AFB - Dallas	212	25
Reese AFB - Dallas	265	14

Table I. Percentage of times when $CMSI_i$ gave larger errors than the Billiken-factor method during winter. Note the general decay of these percentages with distance as the joint relationships between stations approach independency. Here a criterion that each of the unconditionals must exceed 2% was invoked to enhance the reliability of the statistics.

The first term in the revised version of equation 31 was found to be nearly a straight line when plotted on semi-log paper which could be represented by the equation 0.216 ln S - 0.347 where S is arbitrarily bounded by $7 \leqslant S \leqslant 400$ miles. These limits impose no restrictions on the usages of the function in actual practice since values in excess of 400 miles can be assumed to be independent. The Billiken factor for the seven mile range was used for distances ranging from 0 through 6 miles as well to avoid blow-ups as the function in equation 32 approaches zero.

The complete revised analytic function then becomes

$$BF = 0.216 \ln S - 0.347 + \frac{0.0041\ S}{\exp(S/115)} \times \cos\left(\frac{(m+5)\pi}{6}\right). \quad (32)$$

6) Verifications on Dependent Data

The analytic formulation was tuned to encompass the independent station pairs listed in Table I and the original 39 pairs of stations used to derive equation 31. Table II presents verification statistics on a representative portion of the originally dependent sample. This table shows that certain routes of short distances such as Travis to Alemeda, for instance, fit the analytic function less well than others. Often weather at one station comprising the route may be extremely localized due to orographic or topographic effects. Hence its dependency characteristics with respect to other stations represent an anomaly from the climatic group. In such instances forecast MSI's should be more heavily relied upon than their modelled climatic counterparts. It should be possible to identify such anomalous routes for special consideration in the planning decision process from a knowledge of the location and topography of the stations involved.

Table III is based upon January data and provides magnitude estimates of the improvements over the independent assumption method made by using the revised Billiken-factor techniques.

7) Conclusion

The analytic functions of either equations 31 or 32 represent a convenient method for estimating $CMSI_t$ without having to resort to tracing the data throughout the records of the various stations involved. Either method can be expected to consistently show improved results over the assumption of independency, particularly when stations are situated close together and exhibit high frequencies of non-localized bad weather.

Route	Distance (nm)	Month-January
Mildenhall- Lakenheath	4	100
Travis AFB - Alameda	34	65
Ft. Hood - Bergstrom AFB	52	100
Ramstein - Rhein Main	52	100
Andrews AFB - Dover AFB	68	100
W. Robins AFB - Dobbins AFB	90	100
Altus AFB - Tinker AFB	102	100
Pope AFB - Charleston	145	71
Charleston - W. Robins	181	88

Table II. Verification statistics for select routes which helped provide the original data used to devise equation 31. The numbers denote the percentage of times when CMSI$_i$ gave larger errors than the Billiken-factor method. A criterion was invoked to enhance the reliability of the statistics.

The research so far pertains to flights between two stations. As more stations become involved the method will need to specify when to use the independent assumption and when to assume dependency relationships in a manner somewhat akin to that shown by example 2 of this report. The details of these incorporations will constitute the thrust of subsequent research efforts.

Route	Distance (nm)	Col. 1	Col. 2
Washington, D.C. - Bolling	1	0.4	2.8
Bolling - Andrews	7	0.8	3.7
Washington, D.C. - Andrews	8	0.5	2.5
Randolph - San Antonio	10	1.2	8.1
Kelly - San Antonio	11	0.5	7.6
Randolph - Kelly	18	0.6	7.0
Ft. Hood - Waco	45	0.9	5.7
San Francisco - Sacramento	75	0.5	2.5
Ft. Hood - Randolph	95	1.2	5.0
Kelly - Ft. Hood	108	1.5	4.4
San Antonio - Corpus Christi	118	1.0	3.1
Ft. Hood - Dallas	118	0.7	2.9
Reese - Dyess	131	0.9	2.4
Ft. Hood - Dyess	132	1.4	3.3
Randolph - Waco	136	1.8	4.8
San Antonio - Waco	140	1.2	4.1
Dyess - Dallas	154	0.6	1.6
Waco - Victoria	167	1.4	4.2
Dyess - San Antonio	188	0.4	1.2
Randolph - Dallas	212	1.6	2.7
Reese - Dallas	265	0.5	1.1

Table III. The mean errors (in per cent) between the revised analytic Billiken-factor method and the true CMSI during January are shown in Column I. The mean errors (in per cent) between the independent assumption method and the true CMSI are similarly given in Col. 2.

III. MODELLING THE RUSSWO DATA

Attempts were made to model the ETAC Revised Uniform Summary of Surface Weather Observations (RUSSWO) to compact the voluminous information on ceilings and visibilities which they contained into a minimum of computer statements. We were successful in this attempt since the cumulative alignment of these respective unconditional probabilities present the data in a form amenable to isoline analyses. These analyses exhibited the following useful characteristics.

1) The isolines for any given month and hour are relatively smooth and evenly spaced.

2) Their magnitudes and gradients show cyclic annual and diurnal variations.

These two features allow for data interpolations and deductions which lie at the heart of the problem we set out to solve. For example, the abbreviated presentation shown in figure 14 contains a wealth of information about that station. Here one particular ceiling/visibility category (1000/1) has been extracted from the RUSSWO by month and hour. Note the annual trend to the unconditional probabilities from January to July and the marked differences in diurnal trends between the winter and summer season. A similar presentation is shown in figure 15 for a less restrictive ceiling/visibility criterion (500/½). A comparison of these two figures shows a large decrease in ceiling/visibility probabilities from the higher to lower category. These two specific ceiling/visibility criteria were chosen since they lie close to the diagonal extending outward from the lower right-hand corner of the RUSSWO sheet occupied by the zero percent bad weather (100% good weather). Consequently, a knowledge of these particular unconditional probability values defines the gradients of the isolines of probability of occurrences to permit interpolations to obtain values for nearby categories of ceiling and visibilities. That is, the characteristic behavior of these two select categories reflects those for neighboring categories, as well, with sufficient accuracy to obviate the need for modelling a massive array of information at many points to deduce the field array of ceiling/visibility information contained in the RUSSWO. Hence, ceiling/visibility probability estimates for categories other than 1000/1 and 500/½ were deduced by regression equations of the

$$Y = P\,(500/\tfrac{1}{2}) - B\,[P\,(1000/1) - P\,(500/\tfrac{1}{2})] \ .$$

Here Y is occurrence probability for the ceiling/visibility category desired and B is an empirically derived function. The results indicate that it is possible to estimate reasonably accurate probabilities for any category ≤ (1000/1) from

Month	Local hour 0-2	3-5	6-8	9-11	12-14	15-17	18-20	21-23
J	16.6	17.5	18.0	18.0	17.1	16.5	16.4	17.2
F	17.4	17.2	17.1	17.4	16.7	15.7	15.9	16.0
M	18.9	18.8	19.7	19.0	18.7	19.0	18.5	18.4
A	21.3	22.2	22.0	18.3	15.4	16.2	19.3	20.3
M	22.6	24.9	22.4	18.4	14.2	14.7	18.8	21.8
J	25.9	30.0	25.3	16.8	12.7	12.5	18.6	22.1
J	29.8	34.0	28.5	18.4	12.0	11.9	19.5	26.0
A	25.6	28.8	26.3	17.6	11.4	11.7	16.5	20.6
S	21.2	23.0	22.8	16.2	12.0	12.9	17.0	18.5
O	16.2	18.9	18.8	14.1	10.9	12.3	12.8	14.0
N	15.6	15.4	16.4	15.5	13.3	13.3	13.8	15.1
D	15.4	15.4	16.0	15.3	15.6	14.8	14.8	14.4

Fig. 14. Unconditional probabilities of ceilings less than 1000 ft and/or visibilities less than one mile at Otis AFB.

Month	Local hour 0-3	3-5	6-8	9-11	13-14	15-17	18-20	20-23
J	7.1	8.2	8.5	6.3	2.9	1.9	3.0	4.7
F	4.7	7.5	7.4	5.0	2.4	1.7	2.1	2.9
M	2.0	3.1	3.3	2.0	1.0	0.7	1.1	1.3
A	1.3	2.1	2.6	0.9	0.5	0.1	0.3	0.7
M	0.8	1.2	1.0	0.3	0.2	0.3	0.5	0.6
J	0.2	0.7	0.7	0.2	0	0.2	0	0.2
J	0.0	0	0.3	0.1	0	0.1	0	0.1
A	0	0.2	0.1	0	0	0	0	0
S	0.5	0.9	1.3	0.6	0.2	0.1	0.2	0.3
O	1.4	1.8	1.7	0.8	0.4	0.4	0.3	0.8
N	3.3	4.2	4.9	2.6	1.5	1.3	2.1	2.3
D	4.8	6.8	7.1	4.7	2.2	1.7	1.8	2.8

Fig. 15. Unconditional probabilities of ceilings less than 500 feet and/or visibilities less than one-half mile at Otis AFB.

a knowledge of the >1000/1 and >500/½ values (see Figs. 16a, 16b, 16c and 16d).

Having discovered the cyclic nature of the probability values with respect to hour and month and the feasibility of deducing adjacent categories from a knowledge of two strategically chosen ones, our attention was diverted to how best to represent this information in computer format. Here choices in play-offs between accuracy and compactness are involved. Should utmost accuracy be required, it is suggested that values at each of the eight three-hourly grouping be rounded-off and each month's data stored in the computer as a multi-numbered word. For example, the January values at Otis Air Force Base in figure 14 would be entered as the sixteen digit word, 1718181817171617.

The arrays of figures 14 and 15 can be represented by "types" in a still more compacted form. In this regard we suggest that the data be "normalized" by dividing the actual probabilities at each time grouping by the mean of the month. By dividing out the mean, which is an indication of local effects on the observed weather, emphasis is placed on the effects of the solar forcing function which varies with latitude and altitude. This latter effect can be represented by generalized types whose values, when multiplied by the monthly mean, reproduce the probabilities for the particular station involved.

In the preliminary stages of our investigation, data were extracted from the USAF/ETAC Revised Uniform Summary of Surface Weather Observations (RUSSWO) for twenty-five select stations. Two categories were examined: ceilings greater than 1000 ft and visibilities greater than 1 mile and ceilings greater than 500 ft and visibilities greater than 1/2 mile. This gave 96 probabilities for each station (the data for twelve months for eight 3-hourly periods). One such array for each ceiling/visibility category is presented for Otis Air Force Base in figures 14 and 15. Thus, a total of 300 data arrays (12 months x 25 stations) were available for typing in the preliminary aspects of this research. The stations used are listed in Table IV.

Chitose AB, Japan	Loring AFB, Me
Chiang Mai, Thailand	Great Falls, Mont.
Kingsley Fld., Ore.	Andrews AFB, Md.
Astoria, Ore.	Spangdahlem AF, Germany
Spokane, Wash.	Aviano AB, Italy
Seattle, Wash.	Brunswick, Ga.
Whidbey Island, Wash.	Memphis, Tenn.
Walla Walla, Wash.	Beaufort, S. Car.
McGuire AFB, N. J.	Minot AFB, N. Dak.
Ft. Campbell, Ky.	Elizabeth City, N. Car.
K. I. Sawyer AFB, Mich.	Scott AFB, Ill.
Kincheloe AFB, Mich.	Ft. Riley, Kan.
Otis AFB, Mass.	

Table IV. Twenty-five stations used in initial study.

	0-2	3-5	6-8	9-11	12-14	15-17	18-20	21-23
J	87.9	88.5	86.6	87.0	91.4	92.3	91.0	90.1
	89.5	89.3	88.9	88.2	92.4	92.7	92.0	91.3
F	91.8	88.5	86.6	89.9	96.1	96.8	96.8	94.1
	93.2	90.5	88.0	90.2	96.1	96.1	96.2	95.4
M	94.0	89.9	87.4	95.3	99.7	98.6	98.5	97.9
	95.6	93.4	90.5	96.1	99.4	98.4	97.9	97.8
A	98.8	95.1	95.8	99.6	100.0	100.0	100.0	100.0
	98.9	96.5	95.1	99.3	99.9	99.9	99.9	99.6
M	99.1	94.9	98.0	100.0	100.0	100.0	100.0	100.0
	98.2	96.6	97.5	99.8	99.8	99.9	99.9	99.8
J	99.3	95.7	98.4	100.0	100.0	100.0	100.0	100.0
	98.9	98.1	98.3	99.8	99.9	100.0	99.9	99.8
J	100.0	96.7	96.5	100.0	100.0	100.0	100.0	100.0
	99.8	97.1	97.9	99.9	100.0	99.9	100.0	100.0
A	100.0	93.6	94.0	100.0	100.0	100.0	100.0	100.0
	99.5	95.0	96.0	99.8	99.9	100.0	99.9	99.9
S	97.3	90.9	87.1	97.5	100.0	100.0	99.2	98.9
	97.4	92.5	88.7	97.6	99.8	99.7	99.6	98.9
O	93.4	87.0	82.9	91.5	99.6	99.9	99.0	98.0
	92.8	87.4	83.7	92.6	98.5	99.3	98.7	97.2
N	91.1	88.2	86.1	91.2	96.9	96.8	95.8	94.3
	90.4	88.4	86.9	91.8	97.3	96.4	96.2	94.3
D	86.6	85.9	86.6	87.8	90.7	92.1	90.3	89.2
	88.2	87.1	87.8	87.1	91.6	92.5	92.4	89.9

Fig. 16a. Estimated probabilities of ceiling/visibility 200/½ for upper Heyford, England using the equation $P200/\frac{1}{2} = P500/\frac{1}{2} + B_1(P1000/1 - P500/\frac{1}{2})$. The actual values are plotted underneath for comparison purposes.

	0-2	3-5	6-8	9-11	12-14	15-17	18-20	21-23
J	89.1	89.8	87.1	88.2	92.6	93.5	92.1	91.3
	91.2	91.3	91.0	90.5	94.2	94.8	93.6	92.6
F	92.7	89.5	87.7	91.2	97.0	97.5	97.7	94.8
	94.3	91.7	89.4	92.9	97.5	97.3	97.1	95.8
M	95.0	91.0	88.5	96.3	100.0	99.0	99.0	98.8
	96.4	94.4	92.8	97.6	99.7	99.1	98.5	90.5
A	99.5	96.0	96.9	100.0	100.0	100.0	100.0	100.0
	99.1	96.8	96.1	99.4	99.9	99.9	99.9	99.6
M	99.7	95.8	99.0	100.0	100.0	100.0	100.0	100.0
	98.7	97.2	97.9	99.8	99.8	99.9	99.9	99.8
J	100.0	96.8	99.6	100.0	100.0	100.0	100.0	100.0
	99.1	98.1	98.6	100.0	99.9	100.0	99.9	99.8
J	100.0	97.6	97.4	100.0	100.0	100.0	100.0	100.0
	99.8	97.7	98.4	99.9	100.0	99.9	100.0	100.0
A	100.0	94.6	95.2	100.0	100.0	100.0	100.0	100.0
	99.6	96.2	96.8	99.8	99.9	100.0	99.9	99.9
S	97.9	91.8	88.0	98.1	100.0	100.0	99.4	99.2
	97.9	94.0	90.8	98.2	99.8	99.7	99.6	99.0
O	94.4	88.0	84.0	92.5	100.0	100.0	99.5	98.7
	93.7	89.8	86.5	94.1	99.0	99.6	99.0	97.8
N	92.2	89.3	87.2	92.3	97.9	97.6	96.6	95.3
	92.8	90.6	89.3	94.0	98.2	97.3	97.0	95.6
D	87.8	87.2	87.8	89.1	91.8	93.3	91.3	90.5
	89.4	89.0	90.0	89.5	93.8	94.8	93.7	91.7

Fig. 16b. Estimated probabilities of ceiling/visibility 200/¼ for upper Heyford, England using the equation $P200/\frac{1}{4} = P500/\frac{1}{2} + B_2 (P1000/1 - P500/\frac{1}{2})$. The actual values are plotted underneath for comparison purposes.

	0-2	3-5	6-8	9-11	12-14	15-17	18-20	21-23
J	76.0	76.1	73.9	75.4	79.7	80.7	80.7	78.9
	75.3	74.7	74.6	75.1	79.7	80.6	80.9	78.1
F	83.0	79.0	75.7	77.9	86.9	88.0	87.9	86.3
	83.9	78.9	75.5	77.6	86.5	88.9	88.1	87.1
M	84.3	79.5	76.5	85.0	92.4	93.8	92.2	89.4
	83.6	78.8	76.9	84.1	92.0	93.2	92.3	88.3
A	91.5	86.6	84.7	91.7	96.2	97.2	97.3	95.7
	91.5	85.8	83.8	92.1	96.5	97.4	97.1	95.7
M	92.2	86.0	88.0	93.9	97.5	97.9	97.8	96.8
	91.8	84.6	86.4	93.5	97.5	97.5	97.6	96.8
J	90.7	85.3	86.8	94.4	97.7	98.4	97.3	94.8
	90.3	83.7	84.4	94.5	97.9	98.6	97.5	94.9
J	93.9	88.2	87.8	95.0	98.3	99.1	98.3	97.0
	93.4	86.7	87.3	94.7	98.2	91.1	98.2	96.7
A	92.6	84.0	82.6	91.5	97.0	97.8	98.3	96.4
	92.0	82.1	80.4	90.5	97.1	97.9	98.5	97.1
S	90.2	82.4	78.2	90.5	96.3	96.4	95.8	94.4
	90.4	82.4	78.8	90.9	96.9	95.8	95.7	94.2
O	83.7	76.7	72.5	82.0	91.8	94.1	93.2	89.5
	83.6	77.3	73.2	82.0	91.6	94.3	93.4	89.9
N	80.0	77.4	75.7	80.6	87.3	87.7	86.9	84.8
	79.6	78.2	75.6	81.7	87.4	88.3	87.3	85.9
D	74.7	73.7	75.2	75.6	79.8	81.2	80.3	77.0
	74.4	73.8	75.4	75.7	80.4	81.9	80.8	77.6

Fig. 16c. Estimated probabilities of ceiling/visibility 800/½ for upper Heyford, England using the equation $P800/\frac{1}{2} = P500/\frac{1}{2} + B_3(P1000/1 - P500/\frac{1}{2})$. The actual values are plotted underneath for comparison purposes.

	0-2	3-5	6-8	9-11	12-14	15-17	18-20	21-23
J	76.7	76.8	74.0	76.0	80.3	81.3	81.2	79.5
	76.0	76.0	75.4	76.1	80.2	81.1	81.4	78.9
F	83.5	79.5	76.3	78.6	87.4	88.5	88.3	86.7
	84.1	79.6	76.0	78.2	86.6	89.0	88.2	87.2
M	84.8	80.0	77.1	85.6	92.8	94.0	92.5	89.9
	83.7	79.0	77.7	84.2	92.0	93.3	92.5	88.5
A	91.8	87.0	85.3	92.1	96.4	97.3	97.4	95.9
	91.6	86.0	84.3	92.2	96.5	97.4	97.1	95.7
M	92.6	86.4	88.5	94.3	97.6	98.1	97.9	97.0
	92.2	84.9	86.6	93.5	97.5	97.5	97.6	96.8
J	91.1	85.8	87.4	94.8	97.9	98.5	97.4	95.1
	90.5	83.9	84.5	94.5	97.9	98.6	97.5	94.9
J	94.2	88.7	88.2	95.3	98.4	99.2	98.4	97.1
	93.4	87.0	87.4	94.7	98.2	99.1	98.2	96.7
A	93.1	84.5	83.2	92.0	97.2	97.9	98.4	96.6
	92.1	82.8	80.6	90.5	97.1	97.9	98.5	97.1
S	90.6	82.8	78.6	90.8	96.5	96.5	95.9	94.6
	90.8	83.7	79.9	91.0	96.9	95.8	95.7	94.3
O	84.2	77.3	73.0	82.5	92.2	94.4	93.5	89.9
	84.5	79.0	74.9	82.6	91.9	94.4	93.5	90.2
N	80.6	78.0	76.2	81.2	87.8	88.2	87.4	85.3
	81.1	79.3	77.2	82.9	87.7	88.5	87.6	86.6
D	75.4	74.4	75.8	76.3	80.4	81.8	80.8	77.7
	75.0	74.8	76.6	76.7	80.9	83.3	81.5	78.9

Fig. 16d. Estimated probabilities of ceiling/visibility 800/¼ for upper Heyford, England using the equation $P800/¼ = P500/½ + B_4(P1000/1 - P500/½)$. The actual values are plotted underneath for comparison purposes.

A simple model which takes the normalized diurnal unconditional probability curve for any given month and station from the test data, smooths it and labels it as Type 1 was used. All other normalized diurnal unconditional probability profiles were then compared with that type. Those profiles which match the Type 1 curve, within a specified tolerance, were labeled and temporarily removed from the sample. The procedure was repeated by arbitrarily designating another one of the remaining normalized diurnal profiles as Type 2 and matching all the remaining profiles against it. Proceeding in this fashion, iterations were continued until all the diurnal profiles for all stations for all months were typed. A maximum error at any point in the diurnal profile of ±2% was set as the tolerance for fitting these types. That is, a given unconditional probability must be reproduced within an error of 2.0% at every grid point for a type to be selected. For example, if the true value is 10.3% at any given grid point, the regenerated unconditional probability for that point must fall between 8.3 and 12.3 percent.

Figure 17 indicates the number of types which would have been required to reproduce 300 data sets within certain error tolerances. A refinement was introduced into the procedure after all types have been established to be sure that a station's data, which may meet the tolerances set for more than one type, are placed in the one which it fits the best. Further refinements contemplated are to introduce other criteria for determining the best type based upon correlations and least absolute error considerations. Also, we hope to reduce the number of types shown as being required in figure 17 by following more systematic procedures introduced by Lund whereby the first type chosen is representative of the largest number of fits, the second type the next largest number of fits, etc.

PC(%)	No. of Curve Types Required for 500/½	No. of Curve Types Required for 1000/1
1.0	86	150
1.5	44	95
2.0	31	60
2.5	23	34
3.0	15	23

Fig. 17. The number of types required to reproduce the unconditional probabilities for a given RUSSWO ceiling/visibility category for an unlimited number of stations for all months within a given maximum allowable percentage error (PC).

The various types which fit the data of the 25 stations used in this research are shown in figure 18. These types are based upon the criteria that the ceilings were less than five hundred feet and/or the visibilities less than one half mile. Although it is envisioned that a number somewhat larger than thirty might be needed to type the three hundred sixty some stations that we are currently processing for all months of the year, the amount should remain within manageable bounds. The use of types compacts the monthly data for any one station for two ceiling visibility categories into 8 digits of one number.

We are in the process of typing the monthly profiles of some 360 stations for which we have extracted RUSSWO data. These results will be presented in a form amenable for ready operational implementation should the using agencies choose to do so. Furthermore, they should lend credence to our premise that the unconditional probability data can be compacted by several orders of magnitude with a minimum of loss in integrity. A hypothetical example of this might be the number 11070625. Here the number 11 represents twice the value of 5.5 for the 1000/1 profile. The number 07 refers to type 7 which this profile has been found to match by the aforementioned procedures. The number 06 refers to twice the mean value for the 500/½ category and 25 designates the type that matches its diurnal profile. We have chosen to enter twice the mean value to minimize round-off errors occasioned when the normalized values of each type are multiplied by that mean to reproduce the station's original diurnal trace.

Month

STATION	01	02	03	04	05	06	07	08	09	10	11	12
KFMH	1	1	1	2	3	4	4	4	3	2	30	1
KHOP	16	14	7	5	31	31	27	27	27	5	7	16
KADW	16	16	16	2	5	5	27	24	6	6	14	29
KGTF	25	6	28	7	6	6	23	28	6	6	16	14
KINR	25	14	26	30	5	5	5	24	7	9	29	1
KSAW	16	25	8	14	9	7	5	5	14	9	10	29
RJCC	25	3	13	12	13	11	12	13	4	4	1	29
KSFF	14	9	6	23	27	27	27	6	23	15	14	16
KSSI	7	9	6	5	23	6	6	6	23	6	24	9
KAST	3	5	27	31	27	17	17	17	31	5	9	3
KLMT	7	24	7	5	27	27	27	22	22	22	15	7
KECG	3	9	3	17	17	31	27	27	27	31	17	2
KNBC	14	26	7	6	23	22	6	18	23	15	28	14
KELV	10	14	9	5	27	27	27	24	23	6	6	16
VICC	21	6	19	18	13	13	18	18	19	20	20	21
KNQA	8	26	7	23	31	6	15	27	6	6	28	25
KSEA	9	28	23	22	22	23	22	22	22	23	28	9
KFRI	7	7	26	27	27	27	22	22	23	6	6	14
LIPA	30	9	7	5	3	17	19	23	23	24	16	30
KNUW	16	9	24	23	23	24	23	23	24	24	4	9
EDAD	25	26	6	23	27	31	27	5	24	28	14	29
KLIZ	29	1	1	2	4	5	5	6	7	14	1	1
KALW	16	16	7	15	11	17	1	13	13	7	30	30
KWRI	10	10	16	4	5	31	31	31	5	5	9	25
KMIB	26	3	28	26	4	27	22	23	23	9	14	29

Fig. 18. The numbers indicate which of the 31 types best fit the diurnal profile of the listed stations for a given month. The criteria are ceilings less than 500' and/or visibilities greater than 1/2 mile. The match between the diurnal profiles and those of the "type" must be within 2% at every grid point.

References

Gringorten, I., 1971: Modelling conditional probability. Preprints, Intern. Symp. Probability and Statistics in the Atmospheric Sciences, Honolulu, Amer. Meteor. Soc., 156-161.

Lund, I. A. and D. D. Grantham, 1976: A model for estimating joint probabilities of weather events. J. Appl. Meteor. (submitted for publication).

Printed by
United States Air Force
Hanscom AFB, Mass. 01731